NeuroImage 323 (2025) 121519

Contents lists available at ScienceDirect

NeuroImage

journal homepage: www.elsevier.com/locate/ynimg

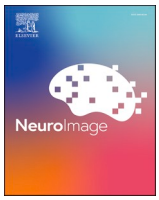

Altered electrophysiological meta-state dynamics in disorders of consciousness

Pablo Núñez [a,b,c,d,*], Prejaas Tewarie [e,f,h], Víctor Rodríguez-González [c,d], Naji L.N. Alnagger [a,b], Glenn J.M. van der Lande [a,b], Marie M. Vitello [a,b], Paolo Cardone [a,b], Aurore Thibaut [a,b], Laouen Belloli [g], Steven Laureys [a,b,h,i], Jacobo D. Sitt [g,1], Jitka Annen [a,b,j,1], Olivia Gosseries [a,b,1,*]

[a] Coma Science Group, GIGA-Consciousness, GIGA Institute, University of Liège, Liège, Belgium
[b] NeuroRehab & Consciousness Clinic, Neurology Department, University Hospital of Liège, Liège, Belgium
[c] Biomedical Engineering Group, University of Valladolid, Valladolid, Spain
[d] Centro de Investigación Biomédica en Red en Bioingeniería, Biomateriales y Nanomedicina, (CIBER-BBN), Madrid, Spain
[e] Clinical Neurophysiology Group, University of Twente, Enschede, the Netherlands
[f] Sir Peter Mansfield Imaging Centre, School of Physics, University of Nottingham, United Kingdom
[g] Institut du Cerveau - Paris Brain Institute - ICM, Inserm, CNRS, Sorbonne Université, Paris, France
[h] CERVO Brain Research Centre, Laval University, Québec, Canada
[i] International Consciousness Science Institute, Hangzhou Normal University, Hangzhou, China
[j] Department of Data Analysis, University of Ghent, Ghent, Belgium

ARTICLE INFO

Keywords:
Dynamic functional connectivity
Resting-state
Auditory local-global paradigm
Metastates
Disorders of consciousness
Minimally conscious state
Unresponsive wakefulness syndrome

ABSTRACT

Background: This multi-centric study aimed to explore differences in brain activity patterns in patients with disorders of consciousness (DoC), including unresponsive wakefulness syndrome (UWS) and minimally conscious state (MCS).

Methods: Using high-density electroencephalographic (EEG) recordings from 368 DoC patients, 39 who emerged from MCS (eMCS), and 73 healthy controls, we examined instantaneous functional connectivity-based meta-states acting as attractors in a dynamical system, extracted by means of community detection algorithms and recurrence analysis. We analyzed data from two patient cohorts and included resting-state and auditory processing tasks in four frequency bands (delta, theta, alpha, beta) and from three perspectives, namely: (i) discrete activation of dominant states, (ii) a dynamical system composed of attractor states and (iii) the correlation and anticorrelation patterns of the active states.

Results: Findings revealed that while the overall structure of brain connectivity remained stable after injury, patients with DoC and those who emerged showed notable differences in the speed and consistency of how their brain states activated. Specifically, in higher frequencies, UWS patients exhibited faster, and less stable dynamics, shorter dwell times and decreased meta-state anticorrelation compared to those in MCS and eMCS. Moreover, a four-way combined learning classification analysis showed that the measures were able to distinguish the UWS and MCS subgroups.

Significance: These brain state dynamics could serve as valuable markers for assessing states of consciousness. Our results highlight the potential of using high-temporal resolution dynamic brain activity patterns to improve the understanding of altered consciousness and their application to clinical settings.

1. Introduction

Survivors of severe brain damage, due to traumatic brain injury (TBI), cardiac arrest, stroke or other causes, can find themselves in a transient state of absence of arousal and awareness, known as coma (Posner et al., 2008). Eventually, patients may recover arousal and sometimes non-reflexive

* Corresponding authors.
E-mail addresses: P.Nunez@uliege.be (P. Núñez), ogosseries@uliege.be (O. Gosseries).
[1] These authors contributed equally to this work.

https://doi.org/10.1016/j.neuroimage.2025.121519
Received 10 January 2025; Received in revised form 6 October 2025; Accepted 8 October 2025
Available online 9 October 2025

behaviours. Patients with vegetative state/unresponsive wakefulness syndrome (VS/UWS) only show reflex movements and eye-opening (wakefulness) (Laureys et al., 2010). Patients in minimally conscious state (MCS) are characterised by increased awareness, as indicated for example, by the presence of eye tracking, localisation to pain, or simple responses to commands (Giacino et al., 2002). These clinical entities (coma, UWS and MCS) are collectively known as disorders of consciousness (DoC) (for reviews see Zasler et al., 2019 and Alnagger et al., 2023). Furthermore, some patients show emergence from MCS (eMCS), which is marked by the recovery of consistent functional communication and/or use of objects (Giacino et al., 2002).

Clinical experts diagnose DoC using standardized behavioural scales and the most recommended is the Coma Recovery Scale-Revised (CRS-R) (Seel et al., 2010). Nonetheless, all behavioural evaluations share a fundamental limitation: a subset of patients with DoC exhibit a dissociation between preserved brain function (revealed through neuroimaging) and their behavioral presentation, leading to potential underestimation of consciousness (Bodien et al., 2024; Claassen et al., 2024; Schnakers et al., 2015). These patients, behaviourally unresponsive (i.e., UWS) but with brain function closer to MCS (referred to as MCS*) (Gosseries et al., 2014) were shown to compose over 50 % of a cohort of UWS patients, and had better outcomes than UWS patients (Thibaut et al., 2021). These findings underscore the significance of employing neuroimaging tools to enhance the diagnosis of DoC, serving as a supplementary resource alongside conventional behavioural assessments (Giacino et al., 2018; Kondziella et al., 2020; Schiff et al., 2014).

It has been shown that even during rest, the brain exhibits continuously evolving, non-stationary network patterns (Demertzi et al., 2019; Hansen et al., 2015). These rapidly switching temporal architectures might be key to understanding the fundamental properties of conscious brain activity. Indeed, pharmacologically-induced loss of consciousness through anaesthesia leads to brain states with reduced connectivity and less recurrent dynamics, which are remarkably similar to those observed in brains with DoC (Barttfeld et al., 2015; López-González et al., 2021; van der Lande et al., 2024). Furthermore, other states of (un)consciousness such as sleep stages and their transitions can be well characterised and distinguished by features of ongoing brain activity (American Academy Of Sleep Medicine, 2023). Therefore, it is reasonable to assume that awareness and wakefulness would also be characterised by specific spatio-temporal brain states and the transitions between them (Barttfeld et al., 2015; Demertzi et al., 2019; van der Lande et al., 2024).

Among the functional imaging techniques used to gain insights into the heterogeneous pathological alterations of dynamic brain function of DoC, electroencephalography (EEG) stands out due to its very high temporal resolution and ability to measure scalp-level neuronal activity directly (Engels et al., 2017; O'Neill et al., 2018). Its diagnostic relevance is evidenced by the European Academy of Neurology's recommendation to use quantitative analysis of high-density EEG for differentiating between UWS and MCS as part of a multimodal assessment (Kondziella et al., 2020).

The dynamic nature of functional interactions between neuronal clusters (functional connectivity, FC) has been emphasised recently due to the increasing evidence that averaging FC over time (static functional connectivity, sFC) may obscure useful information about the dynamic nature of functional connections (Garrett et al., 2013; O'Neill et al., 2018; Waschke et al., 2021). Dynamic functional connectivity (dFC) (Hutchison et al., 2013; O'Neill et al., 2018) fluctuations, measured through fMRI, have been shown to present non-trivial structure compatible with discrete collections of dynamic brain states (Cavanna et al., 2018). Some studies have gained insights into functional brain dynamics associated with altered states of consciousness induced by brain injury mostly through fMRI recordings (Demertzi et al., 2019; Luppi et al., 2019; Panda et al., 2022), and interest in dFC EEG studies has started to emerge in recent years (Bai et al., 2021; Della Bella et al., 2022).

In the present work, we studied brain states using a method designed to extract temporally repeating patterns of brain network configurations acting as metastable attractors (meta-states) (Cavanna et al., 2018), based on high-temporal-resolution instantaneous FC and community detection algorithms applied to EEG recordings. The aim of the study was to uncover the temporal dynamics of these meta-states in DoC and eMCS patients. This could provide insight into how the properties of the inherently dynamic electrophysiological brain activity, such as the stability of the system, are altered in DoC, and use information about these complex dynamics as potential biomarkers for DoC subtypes.

We addressed four key objectives: (i) to extract recurrent brain networks ("meta-states") in prolonged UWS, MCS, and eMCS patients, as well as controls, (ii) to determine whether there are DoC-related alterations to normal meta-state connectivity, (iii) to assess the properties of dynamic meta-state activation at the group level and how DoC conditions potentially alter them; and (iv) to evaluate the diagnostic capabilities of the meta-state activation measures as biomarkers. To this end, we used three different sets of meta-state activation features: based on discrete activation of single dominant states, meta-states as attractors in a dynamical system, and correlation/anticorrelation of the states with the ongoing functional connectivity.

2. Materials and methods

2.1. Subjects

The retrospective study cohort consisted of two independent datasets obtained at the University and University hospital of Liège and the Pitié-Salpêtrière hospital in Paris. The study was approved by the Ethics Committee of the University hospital of Liège and the Pitié-Salpêtrière hospital according to the Declaration of Helsinki. The patients' legal guardians and the healthy controls gave written informed consent. All patients were behaviourally assessed by means of the CRS-R (Giacino et al., 2004). The diagnosis was based on the best CRS-R score out of 3 to 5 assessments. In the Liège dataset, they were performed at least five times, while in the Paris dataset, clinical assessments were conducted a minimum of three times. In all instances, these assessments were administered on different days by trained clinicians.

EEG recordings in the Liège dataset were collected in a resting state, task-free manner (Chennu et al., 2017). Conversely, in the Paris dataset, task-related EEG signals were acquired utilizing the auditory "Local--Global" paradigm (Bekinschtein et al., 2009), which was tailored to investigate both unconscious and conscious auditory processing. This protocol consists of a series of 5 tones, where the last one can be identical (local standard) or different from the previous ones in pitch (local deviant). The protocol also includes a second level regularity defined by the overall frequency of the series of 5 tones (global standard, 80 % of trials; global deviant, 20 % of trials).

The Liège dataset consisted of 132 prolonged (> 28 days post-injury) subjects: 23 UWS patients (including 4 MCS*), 55 MCS patients (17 MCS-, 38 MCS+), 18 eMCS patients and 36 healthy controls. Parts of this dataset were previously used in other studies (Annen et al., 2023; Chennu et al., 2017; Thibaut et al., 2021).

The Paris dataset consisted of 348 prolonged subjects: 145 UWS, 145 MCS (93 MCS- and 52 MCS+), 21 eMCS patients and 37 healthy controls. Parts of this dataset were previously used in other studies (Engemann et al., 2018; Sitt et al., 2014). For more details on the Local-Global paradigm data used here, please refer to Engemann et al. (2018).

The patients' demographic information of both datasets is listed in Tables 1 and 2. Table S1 in the supplementary material shows the differences in demographic parameters between the two datasets. For more information about the databases used in the study, see the supplementary material.

Table 1
Socio-demographic and clinical data for the Liège dataset. Statistically significant between-group differences are marked with asterisks *$p < 0.05$ (Kruskal-Wallis test for age, chi-squared test for sex and aetiology). m: mean; std: standard deviation; M: male; F: female; N/A: not applicable. CRS-R: Coma Recovery Scale – Revised.

	Group			
Data	UWS	MCS	eMCS	Controls
Number of subjects	23	55	18	36
Age (years) (m±std)*	42.39±14.06	41.16±18.62	29.94±11.91	44.27±15.31
Sex (M:F:Missing)	12:11:0	36:19:0	12:6:0	18:17:1
CRS-R total score (m±std)	6.30±1.33	12.61±4	17.64±5.10	N/A
Anoxia (%)*	56.52	17.85	5.55	N/A
Stroke (%)*	4.35	3.57	11.11	N/A
Traumatic brain injury (%)*	21.74	46.43	55.55	N/A
Other (%)*	17.39	25	27.77	N/A
Time since onset (months) (m±std)*	23.26±38.42	40.13±46.53	44.75±76.18	N/A

Table 2
Socio-demographic and clinical data for the Paris dataset. Statistically significant between-group differences are marked with asterisks *$p < 0.05$ (Kruskal-Wallis test for age, chi-squared test for sex and aetiology). m: mean; std: standard deviation; M: male; F: female; N/A: not applicable. CRS-R: Coma Recovery Scale – Revised.

	Group			
Data	UWS	MCS	eMCS	Controls
Number of subjects	145	145	21	37
Age (years) (m±std)*	46.75±17.32	47.21±17.13	47.33±19.09	25.2±4.1
Sex (M:F:Missing)	92:50:3	83:61:1	14:7:0	24:13:0
CRS-R total score (m±std)	4.97±1.53	10.04±2.83	18.24±4.07	N/A
Anoxia (%)*	48.96	24.82	4.76	N/A
Stroke (%)*	20	25.51	23.80	N/A
Traumatic brain injury (%)*	3.44	14.48	14.28	N/A
Other (%)*	27.59	35.17	57.14	N/A
Time since onset (months) (m±std)*	6.11±19.44	7.90±20.59	18.38±32.76	N/A

2.2. Electroencephalographic recordings

The EEG data from both datasets were recorded with a 256-channel high-density EEG system (EGI, Electrical Geodesics Inc.), with a sampling frequency of 250 Hz. Patients and controls subjects remained awake with eyes open during the recordings.

In the Liège dataset, the resting state EEG was acquired for a period of 20–30 min. Data cleaning involved several steps. First, the EEG was filtered using a 6th-order Butterworth high-pass filter at 0.5 Hz and an 8th-order IIR Butterworth low-pass filter at 100 Hz, with notches at 50 and 100 Hz. The EEG data was then segmented into 2.2040-second epochs. Bad channels were rejected based on visual inspection of the raw time series, and bad segments were identified by visual inspection in principal component analysis (PCA) space by transforming the time series into 20 PCA components. Full independent component analysis (ICA) was performed, and components corresponding to non-neural activity were removed. Finally, bad channels were reconstructed by means of spherical interpolation. The data was re-referenced to the average reference, and the first minute of continuous activity without artifacts was kept for all the subjects (Annen et al., 2023; Núñez et al., 2021a, 2021b).

In the Paris dataset, the preprocessing was fully automated. EEG recordings were band-pass filtered from 0.5 to 45 Hz using a 6th and 8th order FFT-based Butterworth filter. The data were then segmented into epochs from −200 ms to 1336 ms relative to the onset of the first sound. Epochs were excluded based on adaptive outlier detection (see Engemann et al. (2015)). Subsequently, the data were re-referenced using an average reference, and baseline correction was applied. The first 40 epochs from Local Deviant Global Deviant (LDGD) trials were kept, similar to how the first 40 trials with attended target tones were kept in Núñez et al. (2022), in order for the resting-state (Liège) and Local-Global (Paris) recordings of each subject to be of similar lengths (61.712 s and 61.76 s, respectively).

The preprocessing steps for both datasets are explained in detail in the previously published studies (Annen et al., 2023; Engemann et al., 2015).

2.3. Magnetic resonance imaging

In the Liège dataset, the structural (T1) MRI images (120 transversal slices, TR = 2300 ms, voxel size = 1.0 × 1.0 × 1.2 mm^3, flip angle = 9°, field of view = 256 mm^2) were acquired on a Siemens 3T Trio scanner (Siemens Inc, Munich, Germany) the same week as the EEG recordings. These images were used for EEG source estimation in this dataset. More information about the source estimation performed using these images can be found in the supplementary material.

2.4. Source localization: minimum norm imaging

The EEG time series at the source level were obtained using the weighted minimum norm estimation (wMNE) method, which employs a linear inverse operator to minimize energy (L_2-norm) while incorporating source weighting to mitigate bias towards superficial currents and enhance detection of deep sources (Lin et al., 2004). An implementation of wMNE is accessible through Brainstorm (Tadel et al., 2011).

Additionally, a forward model was constructed utilizing anatomical information from T1-weighted 3D MRI images for each subject. Anatomical maps, segmented into 5 tissues (gray matter, white matter, cerebrospinal fluid, skull, scalp), were generated using the CAT12 software toolbox (Gaser et al., 2023). A three-layer head model (brain, skull, and scalp) was built using the Boundary Element method based on individual tissue maps with OpenMEEG software (Gramfort et al., 2010). This head model served as the source space, comprising 15,000 sources constrained to be normal to the cortex. Subsequently, the sources were regrouped into 90 cortical regions of interest (ROIs) using the AAL90 atlas (Tzourio-Mazoyer et al., 2002), by averaging sources after flipping the sign of sources with opposite directions (Núñez et al., 2021a).

In the Liège dataset, 73 participants (13 UWS, 33 MCS, 11 eMCS patients, and 16 healthy controls) had usable T1 anatomical MRI images (no high motion levels, acquisition or registration errors) and no missing ROIs from the AAL90 atlas after source estimation due to brain lesions.

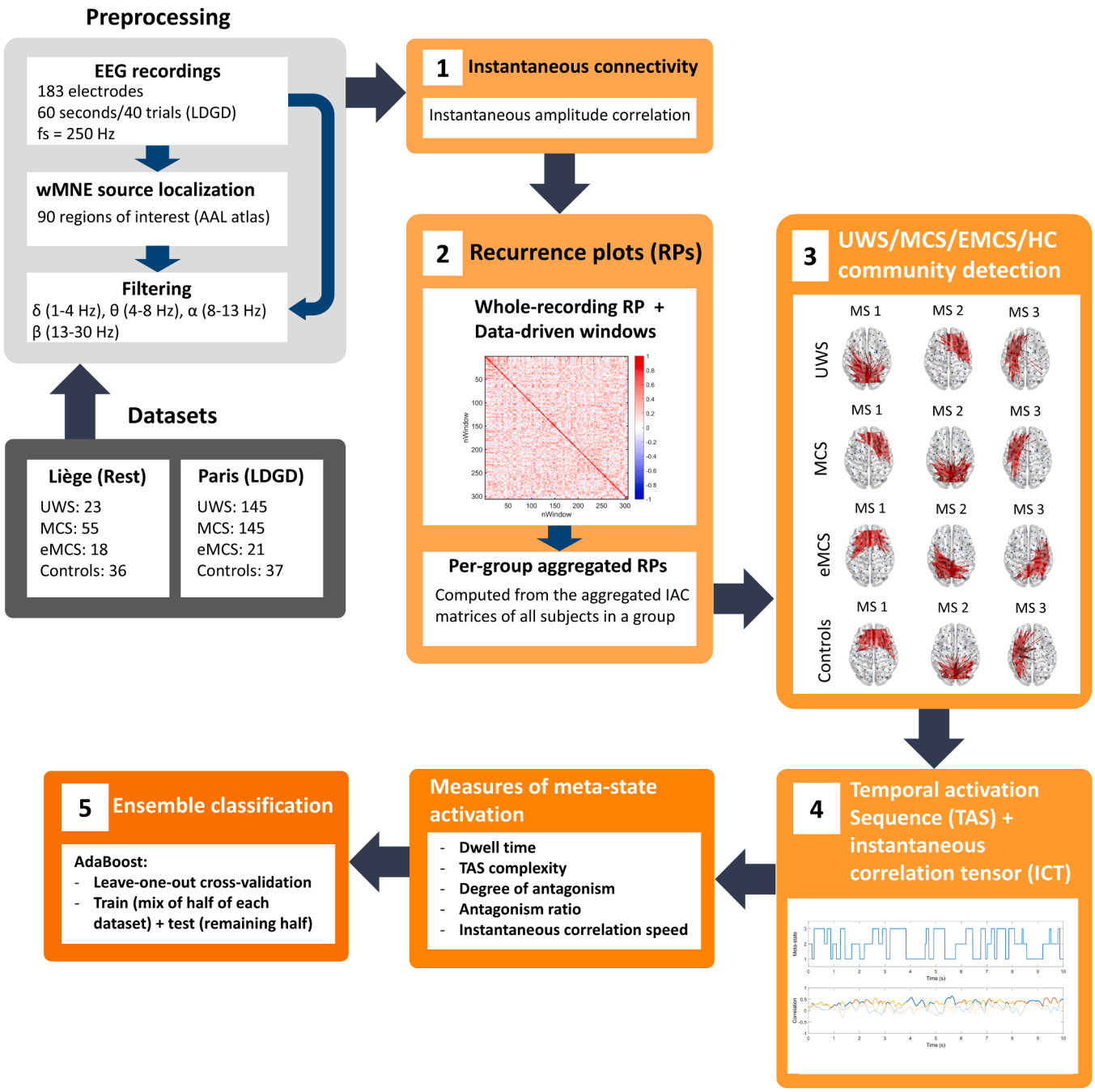

Fig. 1. Meta-state extraction method analysis steps. (1) the instantaneous frequency tensor is obtained by means of the instantaneous amplitude correlation (IAC) in the classical frequency bands: delta (δ, 1–4 Hz), theta (θ, 4–8 Hz), alpha (α, 8–13 Hz), and beta (β, 13–30 Hz). (2) Recurrence plots (RPs) were obtained for the 60-s recordings of each subject by correlating the instantaneous amplitude correlation (IAC) matrices from each temporal sample. Subsequently, data-driven windows were obtained to aggregate the data and reduce the computational burden. (3) Using the data-driven windows, the aggregated individual IAC connectivity tensors of all subjects belonging to a diagnostic group were concatenated and another RP representing the IAC similarity of all the subjects in each group is built. Afterwards, community detection is performed in the RP to obtain the group meta-states. (4) Using the meta-states of the corresponding diagnostic group, the temporal activation sequence (TAS) and the instantaneous correlation tensor (ICT) were obtained for each subject. A variety of measures of meta-state activation dynamics were obtained from the TAS and ICT in each of the frequency bands under study. (5) The measures of meta-state dynamics were fed into an AdaBoost classifier in a LOO—CV procedure for both datasets, as well as trained and tested on a mix of both halves of the Liège dataset and Paris dataset, to determine the best features for group differentiation and the overall diagnostic capabilities of the method in the context of DoC. wMNE: weighted minimum norm estimation. MS: meta state. UWS: unresponsive wakefulness syndrome. MCS: minimally conscious state. eMCS: emergence from minimally conscious state. LDGD: Local Deviant Global Deviant.

2.5. Dynamic meta-state analysis

The main brain meta-state analysis pipeline is based on previously published works (Núñez et al., 2022, 2021a). The principal steps of the method are detailed below and summarised in Fig. 1.

2.6. Instantaneous amplitude correlation (IAC)

The first step of the process consisted of computing a tensor of instantaneous connectivity for every subject by means of the orthogonalized instantaneous amplitude correlation (IAC) in the classical

frequency bands: delta (delta (δ, 1–4 Hz), theta (θ, 4–8 Hz), alpha (α, 8–13 Hz), and beta (β, 13–30 Hz). This frequency separation allows the analyses to acknowledge the inherent functional separation of EEG activity across the spectrum, which could manifest in distinct state dynamics associated to specific bands (Núñez et al., 2022, 2021a).

The IAC is a high-temporal resolution measure of FC, which leverages the EEG's high temporal resolution by giving an index of the amplitude envelope correlation on a sample-by-sample basis (Tewarie et al., 2019). The IAC is obtained as the Hadamard product of the amplitude envelopes of two ROIs i and j (Tewarie et al., 2019).

$$IAC_{ij}(t) = \widehat{E}_i(t) \circ \widehat{E}_j(t) \quad (1)$$

Here, $\circ$ denotes the Hadamard product, and $\widehat{E}(t)$ the amplitude envelope of the z-scored time-series. Due to its sensitivity to signal leakage, a pairwise orthogonalization process was implemented on the time-series post band-pass filtering and before computing the IAC (Brookes et al., 2012; Núñez et al., 2021a; O'Neill et al., 2018; Tewarie et al., 2019).

2.7. Recurrence plots

In the second step, recurrence plots (RPs) were obtained from the IAC matrices corresponding to each temporal sample. RPs are graphical representations that show instances where a dynamical system revisits certain regions within its phase space, aiding in the identification of periodic patterns (Marwan et al., 2007; Tewarie et al., 2019; Webber and Zbilut, 2005).

In this study, as in Núñez et al. (2021a, 2022), we employed the Spearman correlation between the IAC FC time series on each temporal sample to measure the proximity between two points along a trajectory in the RP. We thus define RPs as (Núñez et al., 2022, 2021a; Tewarie et al., 2019):

$$R_{n,m} = corr[IAC(n), IAC(m)] \quad (2)$$

2.8. Data-driven windows

From the RPs, data-driven windows can be derived to aggregate the IAC temporally, utilizing local maxima as boundary points (Tewarie et al., 2019). For more information on the data-driven windows, refer to Tewarie et al. (2019).

The IAC averaged over the data-driven windows enables the computational feasibility of the meta-state detection due to memory constraints in our machines (256 GB of RAM). Due to the high number of subjects in the Paris dataset, 70 patients had to be selected randomly in the UWS and MCS group for the meta-state detection. However, the meta-state activation measures were obtained for all subjects (see section "Measures of meta-state activation").

With the IAC averaged over the windows, "group" RPs were created by concatenating the connectivity tensors of all subjects within a subject group.

2.9. Meta-state detection

We utilised the group meta-states to obtain representations of the temporal dynamics of meta-state activation for each subject. We used the group RPs representing the similarity of IAC windows over time as a weighted graph, with nodes representing data-driven windows of aggregated IAC and edges indicating Spearman correlation values between them. We applied the Louvain GJA community detection algorithm (Gates et al., 2016) to the "group" RPs to detect communities among the connectivity windows, which were identified as meta-states. Given the non-deterministic nature of Louvain GJA, the algorithm was executed 100 times, selecting the solution with the highest modularity (Blondel et al., 2008; Gates et al., 2016; Núñez et al., 2022, 2021a).

The method is described in more detail in Núñez et al. (2021a) and the implementation that can be applied to task data in Núñez et al. (2022).

2.10. Temporal activation sequence and instantaneous correlation tensor

The sample-by-sample IAC FC tensors were correlated with the group meta-states, and each temporal sample was assigned to the nearest meta-state based on Spearman correlation distance. This process generated the Temporal Activation Sequence (TAS), a symbolic time series indicating the most active meta-state at each time point in the recording (Baker et al., 2014; Cabral et al., 2017; Gohil et al., 2022; Núñez et al., 2022, 2021a).

The instantaneous correlation tensor (ICT) represents the Spearman correlation of the IAC FC matrices with each group meta-state for each temporal sample: it therefore has a size of $M \times N$, where M is the number of group meta-states and N is the number of temporal samples (Núñez et al., 2022, 2021a).

Fig. 2 shows the alpha band TAS and the ICT corresponding to a 10 s segment from a control subject during a resting state recording.

2.11. Measures of meta-state activation

A series of measures to characterise the dynamic activation of the meta-states were extracted from the TAS and the ICT. We used a variety of measures characterizing different aspects of the state dynamics in the classical EEG frequency bands (delta, theta, alpha, beta). The measures addressed three key points of the brain state dynamics: (i) from a discrete perspective, i.e., a single state is active at a time (dwell time, TAS complexity), (ii) from the perspective of a dynamical system composed of attractor states (mean and standard deviation of the instantaneous correlation speed), and (iii) from the perspective of the correlation/anticorrelation of states (degree of antagonism, antagonism ratio). Taken together, these metrics provide complementary information about the temporal structure of meta-state dynamics (Núñez et al., 2021a).

Average dwell time: This parameter quantifies the mean duration or lifetimes of the dominant meta-states throughout the recording.

TAS complexity: This metric characterises the structural complexity of meta-state sequencing and is determined by the Lempel-Ziv complexity of the TAS (Abásolo et al., 2006; von Wegner et al., 2024). Higher values denote greater data complexity, indicative of the variety of potential state sequences and their frequencies of occurrence (Núñez et al., 2021a).

Instantaneous correlation speed (ICS): This measure of dynamic stability is directly derived from the ICT. By conceptualizing the ICT as a time-varying position vector, the Spearman correlation of each meta-state can be interpreted as a coordinate in state space. Thus, the ICT measures the dynamic attraction that the meta-states exert on the instantaneous FC over time. The ICS is computed as the temporal derivative of the ICT (Núñez et al., 2021a). Both the mean and the standard deviation of the ICS were obtained, to describe both the average speed of the dynamical system and how dynamically the speed varied in the attractor space.

Degree of antagonism: the degree of antagonism is a measure of the distance between the correlation of the dominant meta-state at each temporal sample and the meta-state with the highest negative correlation. It is intended as a measure of the difference in the strength of the most attractive (correlated) and the most repelling (anti-correlated) attractors in the dynamical system of instantaneous FC, with higher values indicating a more strongly defined dominant state. It is described as:

$$DA = \frac{1}{N}\sum_{n=1}^{N}[PC_{max}(n) + NC_{max}(n)] \quad (3)$$

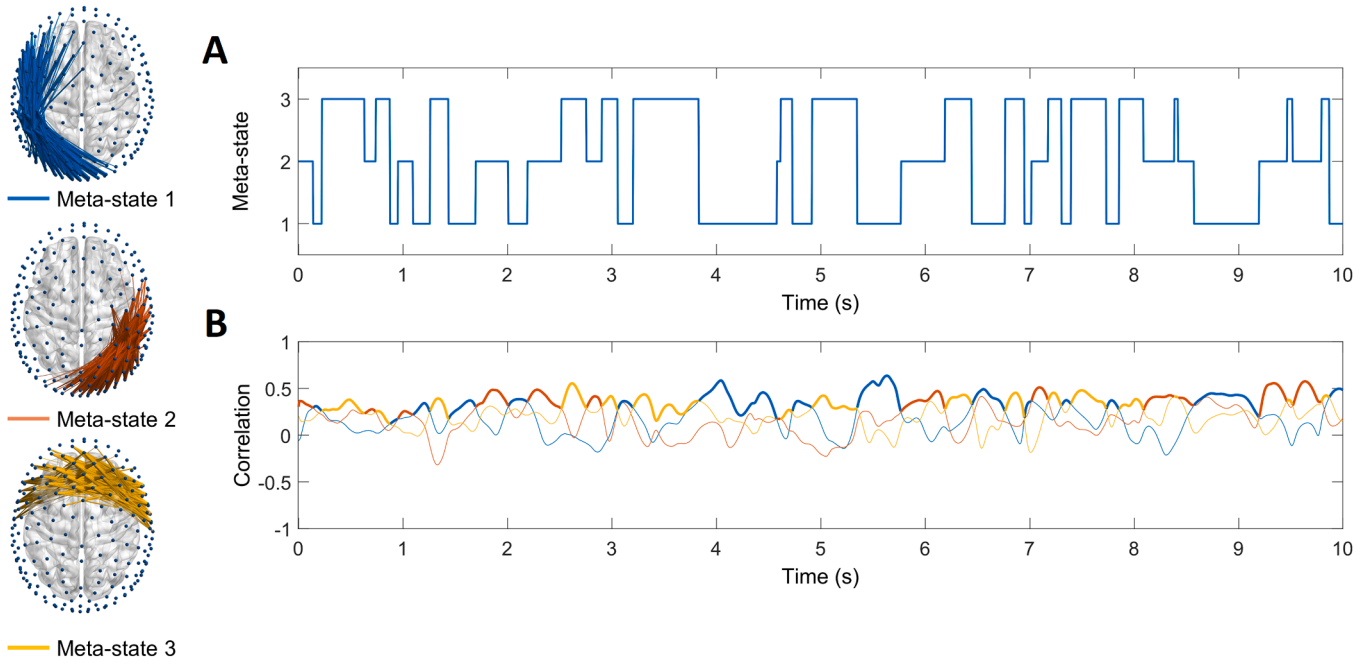

Fig. 2. Temporal activation sequence (A), and instantaneous correlation tensor (B) in the alpha band, both derived from a 10-second segment of resting state activity from a control subject in the Liège dataset. The group meta-states for the control group in this band are displayed to the left.

where $PC_{max}(n)$ is the highest positive correlations in the ICT for temporal sample n, and $NC_{max}(n)$ is the highest negative correlation in the ICT for temporal sample n. Since $NC_{max}(n)$ has a negative value the stronger both $PC_{max}(n)$ and $NC_{max}(n)$ are, the higher the degree of antagonism. In the absence of negative correlations, the degree of antagonism is set to 0.

Antagonism ratio: the ratio between the sum of the absolute value of all anticorrelations and the absolute value of the correlations of all meta states for each temporal sample. The antagonism ratio is defined as:

$$AR(n) = \frac{\sum |NC(n)|}{\sum |NC(n)| + |PC(n)|} \tag{4}$$

where $NC(n)$ are the negative correlations in the ICT and $PC(n)$ are the positive correlations in the ICT. The primary aim of this measure is to evaluate the degree of repulsive forces influencing the ICT. High antagonism ratio can be interpreted as indicative of heightened meta-state anticorrelation or overall low levels of positive correlations of the meta-states compared to negative ones (Núñez et al., 2022).

2.12. Statistical analyses

To check for possible differences in socio-demographic information between the four groups, Kruskal-Wallis tests were conducted to determine global effects, except for sex and aetiology (TBI, anoxia, stroke, other), which were compared by means of chi-squared tests. For the measures of meta-state activation, Kruskal-Wallis tests were used to detect global interactions between the four groups for all measures and frequency bands, after determining that many of the measures did not fulfil the requirement of normality for parametric tests (Shapiro-Wilk test, see supplementary material Tables S2 and S3). If interactions were found, Mann-Whitney U tests were performed to examine possible between-group differences. A false discovery rate (FDR) correction was implemented to adjust for the number of bands in the comparisons (Benjamini and Hochberg, 1995). The significance level was set at α=0.05. Statistical analyses and signal processing were performed using MATLAB® (version R2021a Mathworks, Natick, MA). Brain networks were visualized with BrainNet Viewer (http://www.nitrc.org/projects/bnv/) (Xia et al., 2013).

2.13. Classification with meta-state EEG biomarkers

After extracting all meta-state activation measures, a series of classification analyses were conducted to evaluate their discriminatory abilities and potential use as biomarkers. As in the previous analyses, all meta-state activation measures were obtained from group meta-states. We explored the possibility of using support vector machines (SVM) and linear discriminant analysis (LDA) for classification, but decided to employ multi-class AdaBoost as the classifier with 500 weak learners due to the fact that it includes implicit feature selection in addition to robust classification performance. This enabled us to observe the features that contribute the most to group differentiation. For more information about AdaBoost, please refer to Hastie et al. (2009). We utilized shallow trees with a maximum number of splits equal to 10 as the weak classifier to implicitly perform feature selection within each iteration.

Initially, a leave-one-out cross-validation (LOO—CV) procedure was conducted within the Liège dataset and both trial types in the Paris dataset to estimate classification robustness. Afterwards a combined learning approach was carried out by training a single AdaBoost classifier using a mix of half the subjects from each diagnostic group in both datasets (50 % from the Liège dataset and 50 % from the Paris dataset). The classifier was then used to classify the remaining half of the subjects in both datasets. This process was repeated 100 times, with random permutations of the subjects from each diagnostic group assigned to the training and testing groups. Receiver operating characteristic (ROC) curves were obtained for all classification analyses.

3. Results

3.1. Meta-state detection

EEG recordings from 368 patients with DoC, 39 eMCS patients, and 73 healthy controls were analysed. Per-group community detection was performed on each diagnostic group and frequency band. Meta-state

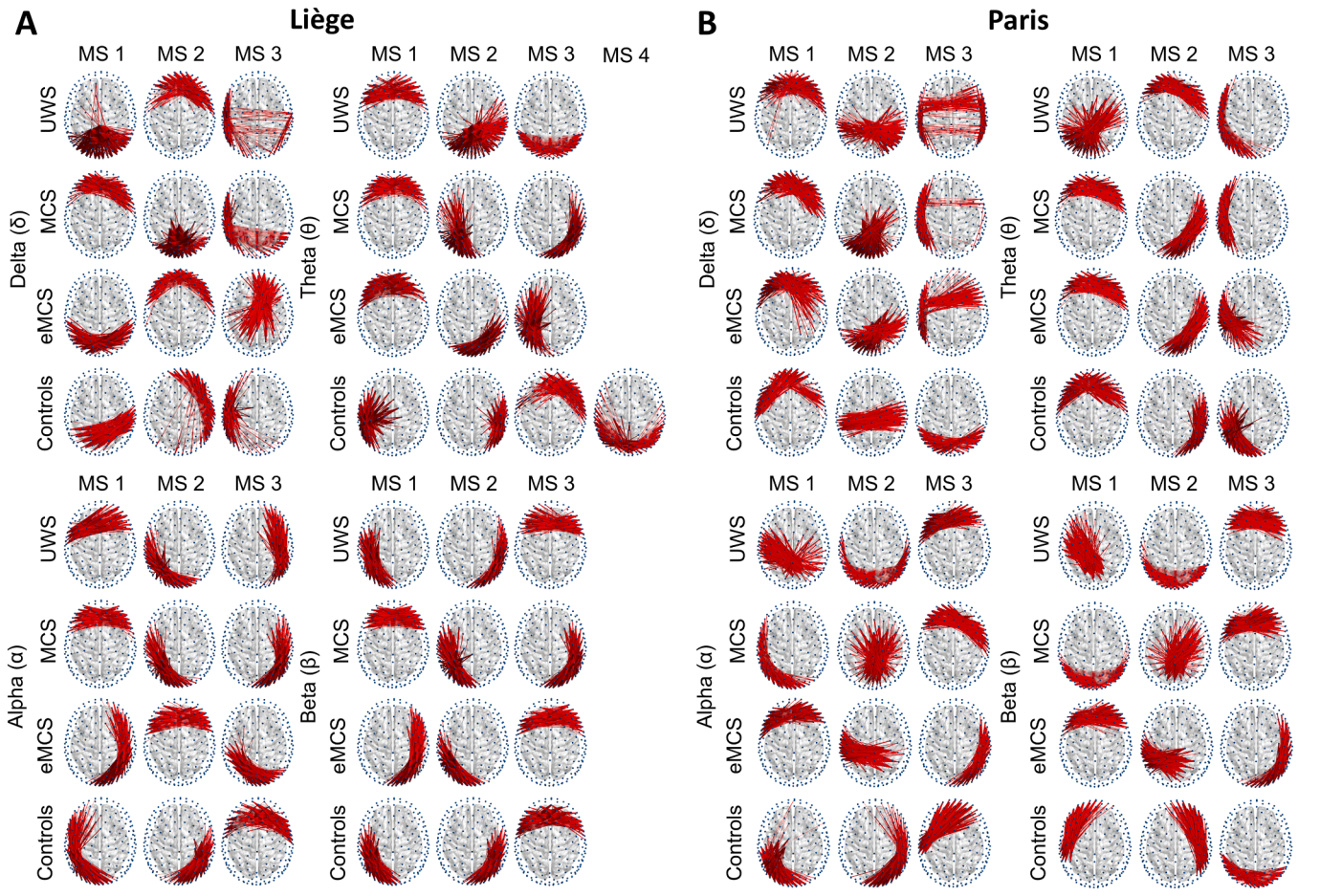

Fig. 3. Brain plots depicting group meta-states (MS) in the (A) Liège dataset and (B) Paris dataset. Only the top 2.5 % strongest connections are displayed. Meta-states were ordered based on their overall frequency of occurrence throughout the recordings in each group. UWS: unresponsive wakefulness syndrome. MCS: minimally conscious state. eMCS: emergence from minimally conscious state.

detection was also performed at the source level using the AAL90 atlas in the Liège dataset (see supplementary material Fig. S1) and to all the subjects of the Liège dataset grouped together as a single group (see supplementary material Fig. S2). Fig. 3 shows the meta-states for all bands in both datasets. Three states were found for each diagnosis with some variations. The meta-states mostly corresponded to a frontal, parieto-occipital and a fronto-occipital network (in either the right or left hemisphere depending on the condition and band), which is in line with previous studies using this method (Núñez et al., 2022, 2021a). In the Paris dataset, while the meta-states largely followed the same patterns of frontal, parieto-occipital and fronto-parietal networks, in some cases different networks could be observed.

3.2. *Between-group comparisons in meta-state activation*

Statistically significant differences between the groups were found for all the measures in the Liège dataset. Significant differences between the groups were also found in the Paris dataset for all measures. The between group-comparisons were also performed at the source level in the Liège dataset for the subjects who had usable T1 images (see supplementary material Fig. S3 and Table S4) and using the meta-states obtained from all the subjects considered as a single group in the Liège dataset (see supplementary material Fig. S4), and the measures showed similar tendencies to those at the electrode level.

Fig. 4 shows the between-group comparisons of the seven measures of meta-state activation in the Liège and Paris datasets. Tables 3 and 4 display the FDR-corrected *p*-values of the Kruskal-Wallis tests to detect interactions among the 4 groups for the Liège and Paris datasets, respectively. The *p*-values of the Mann-Whitney U tests for the *post hoc* between-group pairwise comparisons in those bands that displayed statistically significant interactions can be found in Tables S5–28 in the supplementary material. Additionally, given the significant differences in onset time for the UWS and MCS groups between the datasets, we also studied its effects on the measures. To this end, the subjects were separated into two groups (<1 year since onset, >1 year since onset) and the measures were compared between groups for both datasets. The results are shown in Tables S29 and S30 in the supplementary material. None of the measures showed any significant differences when comparing between these two groups, except the mean of the ICS in the beta band in the Paris dataset.

Additionally, given the statistical differences in aetiology between diagnostic groups in both datasets, we performed the same comparisons using the aetiology (anoxia, traumatic brain injury (TBI), stroke and other) to determine whether significant effects could also be found between these groups, potentially influencing the comparisons. The results are shown in supplementary material Fig. S5. The results indicated that for the mean and SD of the ICS, degree of antagonism and antagonism ratio, there were significant group effects for both datasets, and the Paris dataset also presented group effects in the average dwell time and TAS complexity. In general, the alpha and sometimes beta bands displayed a tendency for the TBI, stroke and "other" groups to have values closer to a state of higher consciousness (MCS, eMCS) while the anoxia groups displayed values closer to those of UWS.

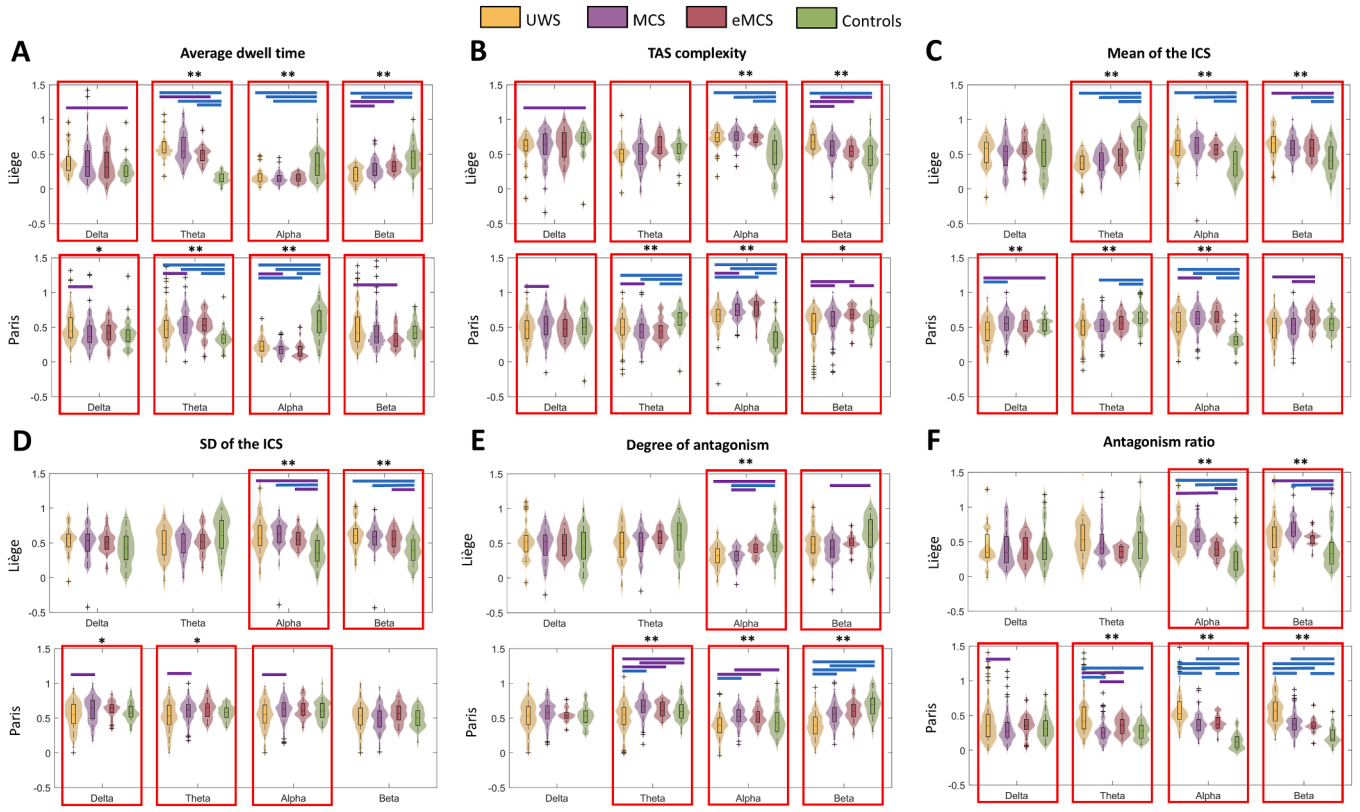

Fig. 4. Distribution plots depicting the (A) average dwell time, (B) TAS complexity, (C) mean of the instantaneous correlation speed (ICS), (D) standard deviation of the ICS, (E) degree of antagonism, (F) antagonism ratio of the Liège and Paris datasets. Red rectangles highlight statistically significant global interactions, i.e., when an effect was found between all three groups, ($p < 0.05$, Kruskal-Wallis test, FDR corrected by the number of bands), while coloured lines denote statistically significant post-hoc pairwise differences, i.e., when differences between two groups were detected ($p < 0.05$, Mann-Whitney U test, FDR corrected by the number of comparisons within the band). In the global interactions, an asterisk (*) indicates a significance level of $p < 0.01$ and two asterisks (**) indicate a significance level of $p < 0.001$. In the pairwise comparisons, purple lines indicate a significance level of $p < 0.05$ and blue lines indicate a significance level of $p < 0.001$. All measures were normalised between 0 and 1 (excluding outliers) in each band for display purposes only. UWS: unresponsive wakefulness syndrome. MCS: minimally conscious state. eMCS: emergence from minimally conscious state. SD: standard deviation.

Table 3
Statistical comparisons for the interactions among the four groups (unresponsive wakefulness syndrome, UWS; minimally conscious state, MCS; emergence from minimally conscious state, eMCS; healthy controls) in the Liège dataset (Kruskal-Wallis test). FDR corrected for the number of bands.

	Delta		Theta		Alpha		Beta	
	$\chi2$	*p*-value	$\chi2$	*p*-value	$\chi2$	*p*-value	$\chi2$	*p*-value
TAS complexity	8.553	0.046	8.014	0.046	30.371	< 0.001	23.643	< 0.001
Average dwell time	8.108	0.044	76.994	< 0.001	31.847	< 0.001	28.723	< 0.001
Mean of the ICS	0.916	0.821	49.005	< 0.001	30.75	< 0.001	16.725	0.001
SD of the ICS	5.220	0.156	6.581	0.115	28.366	< 0.001	25.665	< 0.001
Degree of antagonism	0.842	0.839	3.600	0.411	27.184	< 0.001	15.036	0.004
Antagonism ratio	0.101	0.992	7.449	0.079	58.038	< 0.001	30.909	< 0.001

Table 4
Statistical comparisons for the interactions among the four groups (unresponsive wakefulness syndrome, UWS; minimally conscious state, MCS; emergence from minimally conscious state, eMCS; healthy controls) in the Paris dataset (Kruskal-Wallis test). FDR corrected for the number of bands.

	Delta		Theta		Alpha		Beta	
	$\chi2$	*p*-value	$\chi2$	*p*-value	$\chi2$	*p*-value	$\chi2$	*p*-value
TAS complexity	9.051	0.029	34.665	< 0.001	91.674	< 0.001	12.148	0.009
Average dwell time	14.899	0.003	38.759	< 0.001	85.618	< 0.001	10.312	0.016
Mean of the ICS	27.507	< 0.001	20.825	< 0.001	71.757	< 0.001	9.721	0.021
SD of the ICS	13.679	0.007	13.677	0.007	10.646	0.018	5.303	0.151
Degree of antagonism	7.517	0.057	42.116	< 0.001	46.609	< 0.001	92.253	< 0.001
Antagonism ratio	8.599	0.035	77.959	< 0.001	154.068	< 0.001	129.077	< 0.001

3.3. Resting state (Liège)

3.3.1. Dwell time and TAS complexity

The theta and beta bands showed opposing patterns of increasing or decreasing values with the state of consciousness. For example, the average dwell times were longer in higher frequency bands in controls, while UWS patients had longer state times in the theta band, with MCS and eMCS patients displaying intermediate values in both cases. Moreover, there were statistically significant differences between all patients' groups and controls, and individually between UWS and MCS/eMCS in the beta band. The alpha band appeared as a transition band, with all patients' groups displaying shorter dwell times compared to controls. Similar patterns could be observed in the TAS complexity, indicating that the shorter dwell times contribute to increased meta-state activation complexity in the beta band for DoC and eMCS patients. In the alpha band, all patient groups showed higher complexities than the control group. Crucially, statistically significant differences were found between UWS and MCS patients in the beta band.

3.3.2. Dynamic stability

The mean and SD of the ICS indicated that, both at the source and electrode level, controls displayed slower speeds and decreased speed variability in meta-state space compared to patients in the alpha and beta bands, with the source recordings also showing the same effect in the delta and theta bands.

3.3.3. Meta-state dominance

Finally, the measures of dominant meta-state "antagonism" indicated that in the alpha and beta bands the patient groups showed less separation between the correlation of the dominant state and the meta-state with the highest negative correlation with the current instantaneous FC (degree of antagonism). This indicates that controls showed a more dominant and well-defined active meta-state. Interestingly, the antagonism ratio was higher in the patients in both the alpha and beta bands, indicating more negative forces at play in the DoC and eMCS groups.

3.4. Local-Global paradigm (Paris)

3.4.1. Dwell time and TAS complexity

The measures of meta-state activation displayed both similar and different tendencies in the Paris dataset compared to the Liège dataset. For instance, the average dwell times did not decrease or increase with the state of consciousness in the theta and beta bands respectively, but the alpha differentiation between patients and controls was still present. The TAS complexity showed similar tendencies in both datasets in the delta and theta bands, having significant interactions between the groups in the four bands. However, a pattern of increasing complexity with the state of consciousness could be observed in the alpha band that sharply reversed in controls. The beta-band TAS complexity was also different, with a similar pattern to that of the alpha band, in contrast to the pattern of gradual decrease of complexity with consciousness in the resting state. Contrary to the Liège dataset, only the TAS complexity showed statistically significant differences between the UWS and MCS groups in the beta band, but both this measure and the dwell time showed differences in the theta and alpha band, an effect not present in the Liège dataset.

3.4.2. Measures of dynamic stability

The mean and SD of the ICS again showed results that matched the resting state in the theta and alpha band but not the beta band. In particular, the beta band displayed a pattern of increased speed in eMCS patients compared to other groups, and there were almost no differences in variability of the state-space velocity. Statistically significant differences between the UWS and MCS groups were found in the delta and alpha bands for the mean of the SD of the ICS.

Table 5
Confusion matrix of the LOO—CV classification performed on the Liège resting state data. The y-axis shows the clinical diagnosis (UWS, MCS, eMCS, Controls), while the x-axis indicates the prediction of the classifier. Each cell displays the total number, as well as the percentage (in parentheses) of subjects classified within each clinical category. UWS: unresponsive wakefulness syndrome. MCS: minimally conscious state. eMCS: emergence from minimally conscious state.

Group/predicted	UWS	MCS	eMCS	Controls
UWS	9 (39.13)	13 (56.52)	1 (4.35)	0 (0)
MCS	9 (39.13)	44 (80)	2 (3.64)	0 (0)
eMCS	0 (0)	7 (38.88)	10 (55.55)	1 (5.55)
Controls	0 (0)	1 (2.77)	1 (2.77)	34 (94.44)

3.4.3. Measures of meta-state dominance

Finally, the measures of dominant meta-state "antagonism" were similar to those in the Liège resting state in the alpha and beta bands, with controls showing the highest degree of antagonism and lowest antagonism ratio values, with these values gradually decreasing and increasing, respectively, in eMCS and DoC patients. Furthermore, statistically significant differences between UWS and MCS were observed in the theta, alpha and beta bands for both measures.

3.5. Classification

We conducted two classification analyses using an AdaBoost classifier. First, a LOO—CV procedure was performed on the Liège resting state dataset to estimate classification robustness. The resulting confusion matrix is shown in Table 5, while a histogram with the distribution of selected features of the weak learners is displayed in Fig. S6 in the supplementary material. The overall accuracy was 73.485 % with a Cohen's kappa measure of inter-rater reliability (Cohen, 1960) of 0.691. The same procedure applied to the Paris dataset led to a kappa of 0.535, and overall accuracy of 71.264 % (Table 6). Fig. S7 in the supplementary material displays a histogram showing the distribution of selected features from the weak learners. The main difference between the selected features in the Liège and Paris datasets was the preference towards the dwell time in the theta band, SD of the ICS in the alpha band in the former dataset, which was not the case in the latter, where the antagonism ratio in the alpha and beta bands and the TAS complexity in the alpha band were selected more than the other features overall.

In a second step, we combined both datasets by training a model on a 50–50 split of the Liège and Paris datasets and classifying the remaining half, repeating the process 100 times with random permutations of the subjects in each diagnostic group included in each set. The resulting average confusion matrix is shown in Table 7, while a histogram showing the distribution of selected features from the weak learners is presented in Fig. S8 in the supplementary material. The average accuracy was 66.075 % with a kappa of 0.478. Figures S9 and S10 display the receiver operating characteristic (ROC) curves from the leave-one-out cross-validation (LOO—CV) of the Liège and Paris datasets, respectively, while Figure S11 shows the average ROC curve from the combined learning classification. In both datasets, the ROC curves indicate

Table 6
Confusion matrix of the LOO—CV classification performed on the Paris dataset. The y-axis shows the clinical diagnosis (UWS, MCS, eMCS, Controls), while the x-axis indicates the prediction of the classifier. Each cell displays the total number, as well as the percentage (in parentheses) of subjects classified within each clinical category. UWS: unresponsive wakefulness syndrome. MCS: minimally conscious state. eMCS: emergence from minimally conscious state.

Group/predicted	UWS	MCS	eMCS	Controls
UWS	106 (73.10)	37 (25.52)	2 (1.38)	0 (0)
MCS	27 (18.62)	112 (77.24)	6 (4.14)	0 (0)
eMCS	9 (42.86)	11 (52.38)	1 (4.76)	0 (0)
Controls	3 (8.11)	5 (13.51)	0 (0)	29 (78.38)

Table 7
Average confusion matrix of the combined learning of the model performed by training on half of the subjects from each group in the Liège and Paris datasets and testing on the remaining half. The y-axis shows the clinical diagnosis (UWS, MCS, eMCS, Controls), while the x-axis indicates the prediction of the classifier. Each cell displays the total number, as well as the percentage (in parentheses) of subjects classified within each clinical category. UWS: unresponsive wakefulness syndrome. MCS: minimally conscious state. eMCS: emergence from minimally conscious state.

Group/ predicted	UWS	MCS	eMCS	Controls
UWS	52.57 (62.58)	27.98 (32.14)	1.88 (2.24)	0.57 (0.68)
MCS	20.85 (20.85)	74.35 (74.35)	3.38 (3.38)	0.42 (0.42)
eMCS	2.73 (13.65)	12.85 (64.25)	3.13 (15.65)	0.29 (1.45)
Controls	1.93 (5.22)	5.96 (16.10)	1.58 (4.27)	26.53 (71.70)

that healthy controls were reliably classified based on meta-state dynamics, whereas the DoC groups were more difficult to differentiate. In the Liège dataset, classification performance was higher for the eMCS group compared to UWS and MCS, whereas the Paris dataset showed the opposite trend. The combined learning approach yielded ROC curves more similar to those of the Paris dataset, with classification performance decreasing progressively from healthy controls to UWS, MCS, and eMCS.

4. Discussion

In this work, we investigated brain state dynamics in patients with DoC and eMCS. Using a meta-state detection approach on two large EEG datasets (168 UWS, 200 MCS, 39 eMCS, 73 controls), we investigated whether severe brain injury alters the spatial organisation of attractor states, their temporal dynamics, or both. We found that while the spatial architecture of states is largely preserved, DoC patients show marked alterations in activation dynamics, including faster and less stable transitions at higher frequencies, frequency-dependent changes in dwell times and complexity, and a reduced separation between anticorrelated meta-states. Notably, beta-band dynamics reliably tracked states of consciousness, distinguishing controls, MCS, and UWS in a condition-specific manner. These findings suggest that the injured brain retains basic state architecture but loses efficiency in stabilising activation dynamics, with partial preservation in MCS compared to UWS.

4.1. EEG meta-states

EEG microstates (which are not based on FC patterns but on the topography of the scalp maps of single-electrode activity) have been previously used in studies with DoC patients. In particular, the dynamics of the FC patterns of the microstates and their diagnostic capabilities have been assessed (Hao et al., 2024; Li et al., 2024; Manasova et al., 2025). However, a crucial distinction in the present paper is that the brain states themselves were derived from the FC patterns, and thus no assumptions were made on a direct equivalence between EEG power scalp maps and FC states.

Previous works using this algorithm found similar topographies in the meta-states (Núñez et al., 2022, 2021a), and another EEG-based work using *k*-means clustering on healthy controls and DoC patients found 4 states, of which the first 2 also corresponded to frontal and anterior networks (Bai et al., 2021), a result observed before in the literature utilising MEG analyses (Vidaurre et al., 2018). The meta-state topographies of the Local-Global paradigm differed slightly from the resting state ones, where in some cases the networks were centred around clusters outside the usual frontal/temporal/parieto-occipital configurations (e.g., MCS and eMCS meta-states in the beta band). This could be due to the auditory processing manifesting in the appearance of bilateral temporal auditory networks (Bekinschtein et al., 2009).

4.2. Anticorrelated meta-states

Regarding the topographical similarity between healthy controls and brain-injured patients, the results indicate that alterations to normal function after severe brain injuries do not manifest as different electrophysiological configurations. Instead, these changes are reflected in the temporal activation patterns and the strength of these activations. This is exemplified by the widespread differences in meta-state activation measures across all conditions and frequency bands. Similarly, using *k*-means clustering on fMRI data from healthy controls, UWS, and MCS patients, Demertzi et al. (2019) found four main brain patterns, which differed in their temporal characteristics. This is in line with Panda et al. (2022), who also found decreased dwell times and increased stationarity in DoC using non-negative tensor factorisation. Both studies used states obtained from all subjects grouped together (patients and controls). When applying the same principle to the Liège dataset (see supplementary material), we found that most of the statistical differences from the "per group" analysis persisted, further proving the hypothesis that it is the temporal architecture and not the topography of the states that is altered by DoC and eMCS.

There was a greater separation between the strongest positive and negative correlations of the meta-states in controls compared to brain-injured patients. It has been proposed that an important characteristic of consciousness is the presence of anticorrelated activity patterns (Demertzi et al., 2019, 2013; Hao et al., 2024). The Local-Global recordings exhibited even more significant differences, with average values steadily increasing with the state of consciousness in the beta band. This finding suggests that the greater the separation between anticorrelated meta-states, the higher the state of consciousness, a trend that is more evident in the presence of a passive task. This could also be related to previous observations that patients with DoC not only lack anticorrelation but also exhibit pathological hyperconnectivity between fMRI networks (Di Perri et al., 2016). The increased alpha and beta antagonism ratio in DoC, taken in conjunction with the lower degree of antagonism, also indicated low positive correlations of the instantaneous connectivity with the meta-states, which further points to a general lack of brain state separation in these patients.

4.3. Meta-state dwell times and activation complexity

The measures of meta-state dynamics indicate a general increase in state space instability in patients with DoC and eMCS compared to healthy controls. This was evident in the alpha and beta bands resting-state dwell times and TAS complexity. The results are consistent with those observed by Bai et al. (2021), where three out of four states showed longer average dwell times in controls compared to UWS and MCS patients. In their study, the only state with longer dwell times in DoC patients compared to controls was the anterior state, which was dominated by low-frequency activity (delta, theta), whereas the other three states were dominated by alpha and beta bands (Bai et al., 2021).

Our findings suggest a shift in resting-state dynamics towards lower frequencies in brain-injured patients. An increase in relative power at lower frequencies is a common observation in DoC patients, with UWS patients showing higher delta activity than MCS patients (Piarulli et al., 2016; Sitt et al., 2014; van der Lande et al., 2024). We showed that this power shift is also evident at a higher level of abstraction when examining the brain architecture of DoC and eMCS patients, with observable granular differences in the beta band for each group. Furthermore, this result can be linked to observations in acute patients, showing that an increase in beta brain activity is a sign of better prognosis (MCS, eMCS) (Edlow et al., 2021; Forgacs et al., 2017).

It is important to note that the increased TAS complexity in patients

compared to controls does not conflict with the widely observed trend of decreased brain complexity in DoC patients (Sarasso et al., 2021; van der Lande et al., 2024). Here, we analysed the complexity of the time series of state activations, not the raw brain activity itself or the graph-theoretic properties of the networks (Sarasso et al., 2021). Moreover, EEG time series brain complexity is typically derived from the entire frequency spectrum under analysis (Abásolo et al., 2006; Sarasso et al., 2021), whereas here each frequency band was analysed separately. We hypothesize that the decreased state activation complexity in medium to high frequencies in controls compared to the patients is related to the brain's ability to maintain cost-efficient transition networks (Ramirez-Mahaluf et al., 2020; Zalesky et al., 2014). This finding is in line with that of Annen et al. (2023), who found that cortical alpha power was associated with higher metabolism in DoC patients, while the opposite was true in controls. This supports the notion that DoC patients suffer from decreased efficiency when trying to balance an optimal excitability state.

During the Local-Global paradigm, the theta and alpha bands exhibited similar dwell times and TAS complexity values as observed in the resting state. However, the beta band showed an increase in TAS complexity with the level of consciousness, but with a sharp decrease in average values for the controls. This suggests a functional difference in meta-state activation during a passive auditory task specifically in this band, which is not observed in patients with DoC and in eMCS. Since the beta band is related to attention and expectation during auditory sensory processing (Todorovic et al., 2015) and has been linked to novelty processing (Haenschel et al., 2000), the DoC patients might display lower efficiency during the auditory task, reflected in the increased uncertainty in the sequences of meta-states during the auditory processing of the tones. Indeed, the global effect (GD) within the Local-Global paradigm requires awareness of the global structure of the task by means of conscious detection of the violation of high-level expectations, and an ERP deflection around 300 ms can sometimes be observed in some, but not all the MCS patients in response to the global violation (Bekinschtein et al., 2009). We hypothesise that this heterogeneity in the global effect could lead to mixed responses in the meta-state activation, which could lead to a greater uncertainty and the lack of a general monotonic tendency like the one that can be seen in the resting state Liège dataset.

4.4. Meta-state dynamic stability

In both the alpha and beta bands, both the mean and standard deviation of the ICS were higher for DoC and eMCS patients, while in the theta band, the mean was lower. These findings can be linked to the concept of criticality in dynamical systems. It has been suggested that the brain operates optimally near a critical point on the edge of a bifurcation, separating a stable, low-activity equilibrium state from a region of multistability, where multiple ghost attractors correspond to high activity in different brain areas (Deco and Jirsa, 2012; Vohryzek et al., 2020). Coupled with the observed shorter meta-state duration in DoC and eMCS, these results suggest unstable high-frequency meta-state activation in these patients, where meta-states are dominant for a shorter time, while state-space dynamics show erratic behaviour, drifting around quickly between attractors at varying speeds.

If we consider the healthy controls to be at an optimal working point, the results show that DoC dynamics show a shift towards lower frequencies: instead, the theta band presents the slower dynamics that the controls display in the alpha and beta bands. This finding could be mechanistically related to the widely reported power shift towards lower frequencies in DoC patients (Piarulli et al., 2016; Sitt et al., 2014), showing that it is accompanied by a functional frequency shift of the working point of the criticality dynamics.

In the Local-Global task, the mean of the ICS showed widespread differences between groups, with dynamics being faster in DoC patients in the alpha and beta bands, and slower in the delta and theta bands. Given the presence of the passive auditory task, this suggests that the delta and theta bands play a distinct cognitive role where faster dynamics are required. This may be linked to theta oscillations' involvement detecting and processing of deviant stimuli (Fuentemilla et al., 2008; Hsiao et al., 2009).

4.5. Diagnostic capabilities of meta-state dynamics

As expected, the LOO—CV conducted on the individual datasets resulted in an overly optimistic estimation of classification accuracy and kappa when applying a combined learning approach to the model using a mix of both datasets. Nonetheless, the decline in classification accuracy was reasonable given the underlying difference in the task demands from subjects, demonstrating the robustness of the meta-state activation measures as potential biomarkers. Other studies used the Paris dataset with SVM as the classifier (Sitt et al., 2014), the Liège dataset with SVM as the classifier (Chennu et al., 2017), the Liège dataset with heartbeat-evoked response EEG segments, as well as random EEG segments, using random forest as the classifier (Candia-Rivera et al., 2021), as well as both the Paris and Liège datasets (Engemann et al., 2018) to classify DoC patients using a combination of spectral, connectivity, and information-theoretic measures. The Paris dataset was used as well in combination with the FDG-PET metabolic index (Hermann et al., 2021), and autonomic cardiac markers (Raimondo et al., 2017) but these results are thus not directly comparable with the present study. Sitt et al. (2014) obtained an AUC of 0.78 for the UWS-MCS comparison using 8-fold cross-validation on the Paris dataset. Chennu et al. (2017) obtained an accuracy of 74 %, 100 %, and 71 % when classifying UWS, MCS- and MCS+, respectively, using 4-fold cross validated SVM as the classifier, and alpha participation and delta band power as the features. Candia-Rivera et al. (2021) obtained an accuracy of 66.42 ± 7.13 % when using random EEG segments (as opposed to heartbeat-evoked response). Engemann et al. (2018) used a random forest classifier and obtained an AUC of 0.78 when training on the Liège dataset and classifying the Paris dataset (UWS vs. MCS). On the other hand, while we also obtained an average AUC of 0.78 (UWS vs. all and MCS vs. all), our results are not directly comparable with these previous studies since we performed a combined learning approach, not generalization. Supplementary table S31 displays a comparison of our results with these studies. These results suggest that state activation dynamics could provide complementary information to other measures, aiding in the disentanglement of the neural substrates underlying pathological unconsciousness and minimal consciousness. Note that the time since onset in the Paris dataset was shorter on average than in the Liège dataset, and thus the differences between them could also reflect processes such as neuroplasticity, secondary degeneration, or recovery dynamics. Therefore, disease duration could influence the diagnostic capability of the meta-state dynamics. It is also important to point out that we decided to perform a combined learning approach, as opposed to generalisation (i.e., training on one dataset and testing with the other) due to the unbalanced number of subjects, as well as the different nature of the recordings (resting state vs. passive auditory task). Further research is needed to assess the aforementioned potential complementary information to other biomarkers.

In the four-way combined learning classification, meta-state dynamic measures were largely effective in distinguishing between the UWS and MCS subgroups, though some overlap remained, highlighting the challenge of this task. Nonetheless these results point to state dynamics being a potential marker of DoC recovery. Note that while behavioural diagnoses were used to separate the groups in this study, only four UWS subjects in the Liège dataset were identified as MCS* through positron emission tomography (PET) imaging. Therefore, the UWS group could be considered homogeneous, which supports our attempt to contrast it with MCS. The data from the passive auditory task was more effective in distinguishing between the DoC subgroups, particularly by measuring meta-state antagonism. This suggests that the

significance of state anticorrelation as a marker of consciousness is enhanced in the presence of a passive auditory task. Additionally, task-based functional connectivity can be higher than the one found during rest due to the task-evoked synchronized activity, although there this increase seems to be network-dependent (Arbabshirani et al., 2013), which could lead to a better differentiation in state activations, explaining the higher accuracy of the passive task. While classification of the eMCS group remained modest, this likely reflects the small and imbalanced sample size as well as the diagnostic complexity of eMCS, rather than the choice of classifier. eMCS patients have regained some functions, such as functional communication or object use, but still present severe disability in most domains. Moreover, to be diagnosed as eMCS, these behaviours must be observed reproducibly in two consecutive CRS-R assessments. As a result, eMCS patients may overlap with MCS+ patients who display such behaviours intermittently but do not meet the reproducibility criterion. Consistently, eMCS patients in our study were most often misclassified as MCS, highlighting the clinical and neurophysiological proximity of these two groups. Preliminary tests with alternative algorithms (support vector machines, linear discriminant analysis) have yielded comparable results, suggesting that larger and more balanced datasets will be necessary to fully establish the discriminative value of meta-state dynamics. Notably, direct comparison with previous literature is challenging because eMCS patients are typically excluded from most DoC classification studies, both in EEG investigations (Engemann et al., 2018; Sitt et al., 2014) and in other modalities, including glucose PET (Hermann et al., 2021; Stender et al., 2014) and fMRI (Demertzi et al., 2015). Future studies could explore whether meta-state dynamics are more effective in distinguishing UWS from MCS during active tasks, which are increasingly commonly used in clinical practice (Schnakers et al., 2020).

4.6. Limitations

There are several limitations in this study. Firstly, the meta-state detection method employed the Louvain GJA algorithm in the community detection step for consistency with previous studies (Núñez et al., 2021a, 2022). Nonetheless, other algorithms in the literature could potentially be used (Gates et al., 2016). It also remains to be determined whether the brain meta-states identified here have functional significance or are merely representations of the most common EEG FC clusters in the brain (frontal, parieto-occipital, lateral). In addition, cross-sites studies are challenging due to the differences in acquisition parameters or circumstances. Moreover, memory limitations prevented the use of all subjects in the Paris dataset for the detection of meta-states, as well as for the meta-states representing the combination of the four diagnostic groups combined in the Liège, which meant that it had to be assumed that the random sample of subjects accurately represented the meta-states of the whole group. In the same line, the gamma band was not included in the analysis due to substantial memory constraints linked to the group-level recurrence plot computations, which are particularly demanding for higher frequency bands requiring shorter time windows. Although gamma dynamics are relevant given their role in cognitive processes and responsiveness to stimulation in DoC, practical challenges such as high computational load and susceptibility to muscle artifacts in EEG limit their inclusion. Future work with optimized algorithms and improved EEG acquisition may help address these constraints.

Additionally, we found that when separating the patients by aetiology (anoxia, TBI, stroke and other) instead of diagnosis, the results appeared to follow similar tendencies to UWS and MCS/eMCS: anoxia being closer to UWS behaviour, and stroke and TBI being closer to MCS and eMCS, and “other” displaying wider distributions encompassing various diagnoses. These results can be partially explained by the diagnosis groups showing a bias to specific aetiologies in both datasets (in particular, anoxia is more predominant in UWS than in MCS and eMCS). Nonetheless, it remains a limitation that due to this confounding factor, we cannot fully confirm whether the observed effects are due to diagnosis, aetiology, or a combination of both. It remains an interesting future research line to determine the relationship between aetiology and DoC/eMCS diagnosis when it comes to neuroimaging biomarkers.

Finally, regarding diagnostic performance, we note that classification was not the primary goal of this study. While our meta-state measures achieved performance levels comparable to previous reports using the same datasets, they do not yet surpass established EEG biomarkers. Instead, their main contribution lies in offering a novel dynamical perspective on brain activity, capturing temporal stability, dwell times, and antagonistic relationships of functional connectivity states, that complements spectral and connectivity-based approaches. From a neuroscientific perspective, these features could shed light into how neural systems explore and maintain functional configurations over time, and how DoC reflects a breakdown of the balance of flexible state transitions between metastable states. We therefore consider the present findings as a proof-of-concept, suggesting that meta-state dynamics could enrich frameworks for assessing consciousness, rather than replace existing methods. Future studies combining meta-state features with spectral, connectivity, and information-theoretic measures in larger and more balanced cohorts will be necessary to fully establish their clinical utility.

5. Conclusions

We revealed that the functional connectivity architecture of the main attractor states appears to remain mostly unchanged after injury, but there are fundamental differences in the activation of the states in DoC and eMCS patients. These differences include faster more unstable dynamics at higher frequencies and alterations in state dwell times and activation complexity in UWS and to a lesser extent in MCS patients. Additionally, the injured brain shows decreased separation between anticorrelated meta-states. We also demonstrated that the meta-state space dynamics were a reliable indicator of increased states of consciousness in the beta band and differentiated controls from brain-injured patients, as well as UWS and MCS. This effect, however, was, for the most part, only observable in the resting state recordings of the Liège dataset and thus was not replicable under the Local-Global auditory regularity task. Further research is needed to ascertain the replicability of this effect on independent datasets.

Together, the results suggest that in subjects with DoC and eMCS, meta-state dynamics are on average faster in the alpha and beta bands and slower in the theta band compared to healthy controls. It appears that after injury, the brain can maintain the functional properties of its states to some extent but fails to stabilise the system in the same way as a healthy brain, displaying a loss of efficiency manifested in frequency-dependent altered state activation dynamics. However, some of that functionality seems to be partially preserved in MCS patients compared to UWS. This work paves the way for further exploration of EEG-based state dynamics in DoC by leveraging two large datasets to demonstrate fundamental alterations in brain activation dynamics at rest and in response to stimuli.

Data and code availability statement

The data and the analysis code that supports the findings of this study are available from the corresponding authors, upon reasonable request. Due to the sensitive nature of the clinical information, the ethics protocol does not allow open data sharing.

CRediT authorship contribution statement

Pablo Núñez: Writing – review & editing, Writing – original draft, Visualization, Software, Methodology, Formal analysis, Data curation, Conceptualization. **Prejaas Tewarie:** Writing – review & editing, Software, Methodology. **Víctor Rodríguez-González:** Writing – review &

editing, Software, Methodology. **Naji L.N. Alnagger:** Writing – review & editing. **Glenn J.M. van der Lande:** Writing – review & editing, Data curation. **Marie M. Vitello:** Writing – review & editing, Investigation. **Paolo Cardone:** Writing – review & editing. **Aurore Thibaut:** Writing – review & editing, Investigation. **Laouen Belloli:** Data curation. **Steven Laureys:** Resources. **Jacobo D. Sitt:** Writing – review & editing, Resources. **Jitka Annen:** Writing – review & editing, Supervision, Formal analysis, Data curation, Conceptualization. **Olivia Gosseries:** Writing – review & editing, Supervision, Investigation, Resources, Conceptualization.

Declaration of competing interest

The authors declare that they have no known competing financial interests or personal relationships that could have appeared to influence the work reported in this paper.

Acknowledgments

We thank the patients, their families and the control subjects for participating in our study. The authors extend their gratitude to the entire staff of the ICU, Nuclear Medicine and Radiodiagnostic departments at the University Hospital of Liège. We are especially thankful to the members of the Coma Science Group for their assistance with the clinical evaluations. This work was supported by the University and University Hospital of Liège, the Belgian National Funds for Scientific Research (FRS-FNRS), the FNRS PDR project (T.0134.21), the FNRS MIS project (F.4521.23), the FLAG-ERA JTC2021 project ModelDXConsciousness (Human Brain Project Partnering Project) and FLAG-ERA JTC 2023 - HBP - Basic and Applied Research, project BrainAct, the program Investissements d'avenir ANR-10-IAIHU-06, JTC the fund Generet, the King Baudouin Foundation, the BIAL Foundation, the Funds Chantal Schaeck Yolande, the Télévie Foundation, the Mind Science Foundation, the European Commission, the Fondation Leon Fredericq, the Mind-Care foundation, the National Natural Science Foundation of China (Joint Research Project 81471100), the European Foundation of Biomedical Research FERB Onlus, the Horizon 2020 MSCA – Research and Innovation Staff Exchange DoC-Box project (HORIZON-MSCA-2022-SE-01-01; 101131344), by "MICIU/AEI/10.13039/501100011033″ and "ERDF A way of making Europe" through the project PID2022-138286NB-I00, and "CIBER en Bioingeniería, Biomateriales y Nanomedicina (CIBER-BBN)" through "Instituto de Salud Carlos III" co-funded with ERDF funds. NA and MMV are research fellows, OG and AT are research associates, and SL is research director at the F.R.S.-FNRS. JA is postdoctoral fellow at the FWO (1265522N).

Supplementary materials

Supplementary material associated with this article can be found, in the online version, at doi:10.1016/j.neuroimage.2025.121519.

References

Abásolo, D., Hornero, R., Gómez, C., García, M., López, M., 2006. Analysis of EEG background activity in Alzheimer's disease patients with Lempel-Ziv complexity and central tendency measure. Med. Eng. Phys. 28, 315–322. https://doi.org/10.1016/j.medengphy.2005.07.004.

Alnagger, N., Cardone, P., Martial, C., Laureys, S., Annen, J., Gosseries, O., 2023. The current and future contribution of neuroimaging to the understanding of disorders of consciousness. Presse Med. 52, 104163. https://doi.org/10.1016/j.lpm.2022.104163.

American Academy Of Sleep Medicine, 2023. The AASM Manual for the Scoring of Sleep and Associated Events Version 3. American Academy Of Sleep Medicine.

Annen, J., Frasso, G., van der Lande, G.J.M., Bonin, E.A.C., Vitello, M.M., Panda, R., Sala, A., Cavaliere, C., Raimondo, F., Bahri, M.A., Schiff, N.D., Gosseries, O., Thibaut, A., Laureys, S., 2023. Cerebral electrometabolic coupling in disordered and normal states of consciousness. Cell Rep. 42, 112854. https://doi.org/10.1016/j.celrep.2023.112854.

Arbabshirani, M.R., Havlicek, M., Kiehl, K.A., Pearlson, G.D., Calhoun, V.D., 2013. Functional network connectivity during rest and task conditions: a comparative study. Hum. Brain Mapp. 34, 2959–2971. https://doi.org/10.1002/hbm.22118.

Bai, Y., He, J., Xia, X., Wang, Y., Yang, Y., Di, H., Li, X., Ziemann, U., 2021. Spontaneous transient brain states in EEG source space in disorders of consciousness. Neuroimage 240, 118407. https://doi.org/10.1016/j.neuroimage.2021.118407.

Baker, A.P., Brookes, M.J., Rezek, I.A., Smith, S.M., Behrens, T., Probert Smith, P.J., Woolrich, M., 2014. Fast transient networks in spontaneous human brain activity. Elife 3, 1–18. https://doi.org/10.7554/eLife.01867.

Barttfeld, P., Uhrig, L., Sitt, J.D., Sigman, M., Jarraya, B., Dehaene, S., 2015. Signature of consciousness in the dynamics of resting-state brain activity. Proc. Natl. Acad. Sci. 112, 887–892. https://doi.org/10.1073/pnas.1418031112.

Bekinschtein, T.A., Dehaene, S., Rohaut, B., Tadel, F., Cohen, L., Naccache, L., 2009. Neural signature of the conscious processing of auditory regularities. Proc. Natl. Acad. Sci. U. S. A. 106, 1672–1677. https://doi.org/10.1073/pnas.0809667106.

Benjamini, Y., Hochberg, Y., 1995. Controlling the false discovery rate: a practical and powerful approach to multiple testing. J. R. Stat. Soc. 57, 289–300. https://doi.org/10.2307/2346101.

Blondel, V.D., Guillaume, J.-L., Lambiotte, R., Lefebvre, E., 2008. Fast unfolding of communities in large networks. J. Stat. Mech. Theory Exp. 2008, P10008. https://doi.org/10.1088/1742-5468/2008/10/P10008.

Bodien, Y.G., Allanson, J., Cardone, P., Bonhomme, A., Carmona, J., Chatelle, C., Chennu, S., Conte, M., Dehaene, S., Finoia, P., Heinonen, G., Hersh, J.E., Kamau, E., Lawrence, P.K., Lupson, V.C., Meydan, A., Rohaut, B., Sanders, W.R., Sitt, J.D., Soddu, A., Valente, M., Velazquez, A., Voss, H.U., Vrosgou, A., Claassen, J., Edlow, B. L., Fins, J.J., Gosseries, O., Laureys, S., Menon, D., Naccache, L., Owen, A.M., Pickard, J., Stamatakis, E.A., Thibaut, A., Victor, J.D., Giacino, J.T., Bagiella, E., Schiff, N.D., 2024. Cognitive motor dissociation in disorders of consciousness. N. Engl. J. Med. 391, 598–608. https://doi.org/10.1056/NEJMoa2400645.

Brookes, M.J., Woolrich, M.W., Barnes, G.R., 2012. Measuring functional connectivity in MEG: a multivariate approach insensitive to linear source leakage. Neuroimage 63, 910–920. https://doi.org/10.1016/j.neuroimage.2012.03.048.

Cabral, J., Vidaurre, D., Marques, P., Magalhães, R., Silva Moreira, P., Miguel Soares, J., Deco, G., Sousa, N., Kringelbach, M.L., 2017. Cognitive performance in healthy older adults relates to spontaneous switching between states of functional connectivity during rest. Sci. Rep. 7, 5135. https://doi.org/10.1038/s41598-017-05425-7.

Candia-Rivera, D., Annen, J., Gosseries, O., Martial, C., Thibaut, A., Laureys, S., Tallon-Baudry, C., 2021. Neural responses to heartbeats detect residual signs of consciousness during resting state in postcomatose patients. J. Neurosci. 41, 5251–5262. https://doi.org/10.1523/JNEUROSCI.1740-20.2021.

Cavanna, F., Vilas, M.G., Palmucci, M., Tagliazucchi, E., 2018. Dynamic functional connectivity and brain metastability during altered states of consciousness. Neuroimage 180, 383–395. https://doi.org/10.1016/j.neuroimage.2017.09.065.

Chennu, S., Annen, J., Wannez, S., Thibaut, A., Chatelle, C., Cassol, H., Martens, G., Schnakers, C., Gosseries, O., Menon, D., Laureys, S., 2017. Brain networks predict metabolism, diagnosis and prognosis at the bedside in disorders of consciousness. Brain 140, 2120–2132. https://doi.org/10.1093/brain/awx163.

Claassen, J., Kondziella, D., Alkhachroum, A., Diringer, M., Edlow, B.L., Fins, J.J., Gosseries, O., Hannawi, Y., Rohaut, B., Schnakers, C., Stevens, R.D., Thibaut, A., Monti, M., 2024. Cognitive motor dissociation: gap analysis and future directions. Neurocrit. Care 40, 81–98. https://doi.org/10.1007/s12028-023-01769-3.

Cohen, J., 1960. A coefficient of agreement for nominal scales. Educ. Psychol. Meas. 20, 37–46. https://doi.org/10.1177/001316446002000104.

Deco, G., Jirsa, V.K., 2012. Ongoing cortical activity at rest: criticality, multistability, and ghost attractors. J. Neurosci. 32, 3366–3375. https://doi.org/10.1523/JNEUROSCI.2523-11.2012.

Della Bella, G.A., Zang, D., Gui, P., Mateos, D.M., Sitt, J.D., Bekinschtein, T.A., Manasova, D., Sarton, B., Ferre, F., Silva, S., Lamberti, P.W., Wu, X., Mao, Y., Wang, L., Barttfeld, P., 2022. EEG brain states for real-time detection of covert cognition in disorders of consciousness. PsyArXiv 1–21. https://doi.org/10.31234/osf.io/dbzp6.

Demertzi, A., Antonopoulos, G., Heine, L., Voss, H.U., Crone, J.S., De Los Angeles, C., Bahri, M.A., Di Perri, C., Vanhaudenhuyse, A., Charland-Verville, V., Kronbichler, M., Trinka, E., Phillips, C., Gomez, F., Tshibanda, L., Soddu, A., Schiff, N.D., Whitfield-Gabrieli, S., Laureys, S., 2015. Intrinsic functional connectivity differentiates minimally conscious from unresponsive patients. Brain 138, 2619–2631. https://doi.org/10.1093/brain/awv169.

Demertzi, A., Soddu, A., Laureys, S., 2013. Consciousness supporting networks. Curr. Opin. Neurobiol. 23, 239–244. https://doi.org/10.1016/j.conb.2012.12.003.

Demertzi, A., Tagliazucchi, E., Dehaene, S., Deco, G., Barttfeld, P., Raimondo, F., Martial, C., Fernández-Espejo, D., Rohaut, B., Voss, H.U., Schiff, N.D., Owen, A.M., Laureys, S., Naccache, L., Sitt, J.D., 2019. Human consciousness is supported by dynamic complex patterns of brain signal coordination. Sci. Adv. 5, 1–12. https://doi.org/10.1126/sciadv.aat7603.

Di Perri, C., Bahri, M.A., Amico, E., Thibaut, A., Heine, L., Antonopoulos, G., Charland-Verville, V., Wannez, S., Gomez, F., Hustinx, R., Tshibanda, L., Demertzi, A., Soddu, A., Laureys, S., 2016. Neural correlates of consciousness in patients who have emerged from a minimally conscious state: a cross-sectional multimodal imaging study. Lancet Neurol. 15, 830–842. https://doi.org/10.1016/S1474-4422(16)00111-3.

Edlow, B.L., Claassen, J., Schiff, N.D., Greer, D.M., 2021. Recovery from disorders of consciousness: mechanisms, prognosis and emerging therapies. Nat. Rev. Neurol. 17, 135–156. https://doi.org/10.1038/s41582-020-00428-x.

Engels, M.M.A., van der Flier, W.M., Stam, C.J., Hillebrand, A., Scheltens, P., van Straaten, E.C.W., 2017. Alzheimer's disease: the state of the art in resting-state

magnetoencephalography. Clin. Neurophysiol. 128, 1426–1437. https://doi.org/10.1016/j.clinph.2017.05.012.
Engemann, D., Raimondo, F., King, J.-R., Jas, M., Gramfort, A., Dehaene, S., Naccache, L., Sitt, J., 2015. Automated measurement and prediction of consciousness in vegetative and minimally conscious patients. In: ICML Work. Stat. Mach. Learn. Neurosci. Stamlins 2015.
Engemann, D.A., Raimondo, F., King, J.-R., Rohaut, B., Louppe, G., Faugeras, F., Annen, J., Cassol, H., Gosseries, O., Fernandez-Slezak, D., Laureys, S., Naccache, L., Dehaene, S., Sitt, J.D., 2018. Robust EEG-based cross-site and cross-protocol classification of states of consciousness. Brain 141, 3179–3192. https://doi.org/10.1093/brain/awy251.
Forgacs, P.B., Frey, H.P., Velazquez, A., Thompson, S., Brodie, D., Moitra, V., Rabani, L., Park, S., Agarwal, S., Falo, M.C., Schiff, N.D., Claassen, J., 2017. Dynamic regimes of neocortical activity linked to corticothalamic integrity correlate with outcomes in acute anoxic brain injury after cardiac arrest. Ann. Clin. Transl. Neurol. 4, 119–129. https://doi.org/10.1002/acn3.385.
Fuentemilla, L., Marco-Pallarés, J., Münte, T.F., Grau, C., 2008. Theta EEG oscillatory activity and auditory change detection. Brain Res. 1220, 93–101. https://doi.org/10.1016/j.brainres.2007.07.079.
Garrett, D.D., Samanez-Larkin, G.R., MacDonald, S.W.S., Lindenberger, U., McIntosh, A. R., Grady, C.L., 2013. Moment-to-moment brain signal variability: a next frontier in human brain mapping? Neurosci. Biobehav. Rev. 37, 610–624. https://doi.org/10.1016/j.neubiorev.2013.02.015.
Gaser, C., Dahnke, R., Thompson, P.M., Kurth, F., Gaser, C., Ph, D., 2023. CAT – a computational anatomy toolbox for the analysis of structural MRI. bioRxiv. https://doi.org/10.1101/2022.06.11.495736.
Gates, K.M., Henry, T., Steinley, D., Fair, D.A., 2016. A Monte Carlo evaluation of weighted community detection algorithms. Front. Neuroinform. 10. https://doi.org/10.3389/fninf.2016.00045.
Giacino, J.T., Ashwal, S., Childs, N., Cranford, R., Jennett, B., Katz, D.I., Kelly, J.P., Rosenberg, J.H., Whyte, J., Zafonte, R.D., Zasler, N.D., 2002. The minimally conscious state. Neurology 58, 349–353. https://doi.org/10.1212/WNL.58.3.349.
Giacino, J.T., Kalmar, K., Whyte, J., 2004. The JFK Coma Recovery Scale-revised: measurement characteristics and diagnostic utility. Arch. Phys. Med. Rehabil. 85, 2020–2029. https://doi.org/10.1016/j.apmr.2004.02.033.
Giacino, J.T., Katz, D.I., Schiff, N.D., Whyte, J., Ashman, E.J., Ashwal, S., Barbano, R., Hammond, F.M., Laureys, S., Ling, G.S.F., Nakase-Richardson, R., Seel, R.T., Yablon, S., Getchius, T.S.D., Gronseth, G.S., Armstrong, M.J., 2018. Practice guideline update recommendations summary: disorders of consciousness. Neurology 91, 450–460. https://doi.org/10.1212/WNL.0000000000005926.
Gohil, C., Roberts, E., Timms, R., Skates, A., Higgins, C., Quinn, A., Pervaiz, U., van Amersfoort, J., Notin, P., Gal, Y., Adaszewski, S., Woolrich, M., 2022. Mixtures of large-scale dynamic functional brain network modes. Neuroimage 263, 119595. https://doi.org/10.1016/j.neuroimage.2022.119595.
Gosseries, O., Zasler, N.D., Laureys, S., 2014. Recent advances in disorders of consciousness: focus on the diagnosis. Brain Inj. 28, 1141–1150. https://doi.org/10.3109/02699052.2014.920522.
Gramfort, A., Papadopoulo, T., Olivi, E., Clerc, M., 2010. OpenMEEG: opensource software for quasistatic bioelectromagnetics. Biomed. Eng. Online 9, 45. https://doi.org/10.1186/1475-925X-9-45.
Haenschel, C., Baldeweg, T., Croft, R.J., Whittington, M., Gruzelier, J., 2000. Gamma and beta frequency oscillations in response to novel auditory stimuli: a comparison of human electroencephalogram (EEG) data with in vitro models. Proc. Natl. Acad. Sci. U. S. A. 97, 7645–7650. https://doi.org/10.1073/pnas.120162397.
Hansen, E.C.A., Battaglia, D., Spiegler, A., Deco, G., Jirsa, V.K., 2015. Functional connectivity dynamics: modeling the switching behavior of the resting state. Neuroimage 105, 525–535. https://doi.org/10.1016/j.neuroimage.2014.11.001.
Hao, Z., Xia, X., Pan, Y., Bai, Y., Wang, Y., Peng, B., Dou, W., 2024. Uncovering brain network insights for prognosis in disorders of consciousness: EEG source space analysis and brain dynamics. IEEE Trans. Neural Syst. Rehabil. Eng. 32, 144–153. https://doi.org/10.1109/TNSRE.2023.3346947.
Hastie, T., Rosset, S., Zhu, J., Zou, H., 2009. Multi-class AdaBoost. Stat. Interface 2, 349–360. https://doi.org/10.4310/SII.2009.v2.n3.a8.
Hermann, B., Stender, J., Habert, M.O., Kas, A., Denis-Valente, M., Raimondo, F., Pérez, P., Rohaut, B., Sitt, J.D., Naccache, L., 2021. Multimodal FDG-PET and EEG assessment improves diagnosis and prognostication of disorders of consciousness. NeuroImage Clin. 30. https://doi.org/10.1016/j.nicl.2021.102601.
Hsiao, F.J., Wu, Z.A., Ho, L.T., Lin, Y.Y., 2009. Theta oscillation during auditory change detection: an MEG study. Biol. Psychol. 81, 58–66. https://doi.org/10.1016/j.biopsycho.2009.01.007.
Hutchison, R.M., Womelsdorf, T., Gati, J.S., Everling, S., Menon, R.S., 2013. Resting-state networks show dynamic functional connectivity in awake humans and anesthetized macaques. Hum. Brain Mapp. 34, 2154–2177. https://doi.org/10.1002/hbm.22058.
Kondziella, D., Bender, A., Diserens, K., van Erp, W., Estraneo, A., Formisano, R., Laureys, S., Naccache, L., Ozturk, S., Rohaut, B., Sitt, J.D., Stender, J., Tiainen, M., Rossetti, A.O., Gosseries, O., Chatelle, C., 2020. European Academy of Neurology guideline on the diagnosis of coma and other disorders of consciousness. Eur. J. Neurol. 27, 741–756. https://doi.org/10.1111/ene.14151.
Laureys, S., Celesia, G.G., Cohadon, F., Lavrijsen, J., León-Carrión, J., Sannita, W.G., Sazbon, L., Schmutzhard, E., von Wild, K.R., Zeman, A., Dolce, G., 2010. Unresponsive wakefulness syndrome: a new name for the vegetative state or apallic syndrome. BMC Med. 8, 68. https://doi.org/10.1186/1741-7015-8-68.
Li, Y., Gao, J., Yang, Y., Zhuang, Y., Kang, Q., Li, X., Tian, M., Lv, H., He, J., 2024. Temporal and spatial variability of dynamic microstate brain network in disorders of consciousness. CNS Neurosci. Ther. 30, 1–15. https://doi.org/10.1111/cns.14641.
Lin, F.-H., Witzel, T., Hämäläinen, M.S., Dale, A.M., Belliveau, J.W., Stufflebeam, S.M., 2004. Spectral spatiotemporal imaging of cortical oscillations and interactions in the human brain. Neuroimage 23, 582–595. https://doi.org/10.1016/j.neuroimage.2004.04.027.
López-González, A., Panda, R., Ponce-Alvarez, A., Zamora-López, G., Escrichs, A., Martial, C., Thibaut, A., Gosseries, O., Kringelbach, M.L., Annen, J., Laureys, S., Deco, G., 2021. Loss of consciousness reduces the stability of brain hubs and the heterogeneity of brain dynamics. Commun. Biol. 4, 1037. https://doi.org/10.1038/s42003-021-02537-9.
Luppi, A.I., Craig, M.M., Pappas, I., Finoia, P., Williams, G.B., Allanson, J., Pickard, J.D., Owen, A.M., Naci, L., Menon, D.K., Stamatakis, E.A., 2019. Consciousness-specific dynamic interactions of brain integration and functional diversity. Nat. Commun. 10, 4616. https://doi.org/10.1038/s41467-019-12658-9.
Manasova, D., Perl, Y.S., Bruno, N.M., Valente, M., Rohaut, B., Tagliazucchi, E., Naccache, L., Raimondo, F., Sitt, J.D., 2025. Dynamics of EEG microstates change across the spectrum of disorders of consciousness. Brain Topogr 38, 1–12. https://doi.org/10.1007/s10548-025-01142-x.
Marwan, N., Carmen Romano, M., Thiel, M., Kurths, J., 2007. Recurrence plots for the analysis of complex systems. Phys. Rep. 438, 237–329. https://doi.org/10.1016/j.physrep.2006.11.001.
Núñez, P., Gómez, C., Rodríguez-González, V., Hillebrand, A., Tewarie, P., Gomez-Pilar, J., Molina, V., Hornero, R., Poza, J., 2022. Schizophrenia induces abnormal frequency-dependent patterns of dynamic brain network reconfiguration during an auditory oddball task. J. Neural Eng. 19, 016033. https://doi.org/10.1088/1741-2552/ac514e.
Núñez, P., Poza, J., Gómez, C., Rodríguez-González, V., Hillebrand, A., Tewarie, P., Tola-Arribas, M.Á., Cano, M., Hornero, R., 2021a. Abnormal meta-state activation of dynamic brain networks across the Alzheimer spectrum. Neuroimage 232, 117898. https://doi.org/10.1016/j.neuroimage.2021.117898.
Núñez, P., Rodríguez-González, V., Gutiérrez-de Pablo, V., Gómez, C., Shigihara, Y., Hoshi, H., 2021b. Effect of segment length, sampling frequency, and imaging modality on the estimation of measures of brain meta-state activation: an MEG/EEG study. In: Proceedings of the 43rd Annual International Conference of the IEEE Engineering in Medicine and Biology Society Conference.
O'Neill, G.C., Tewarie, P., Vidaurre, D., Liuzzi, L., Woolrich, M.W., Brookes, M.J., 2018. Dynamics of large-scale electrophysiological networks: a technical review. Neuroimage 180, 559–576. https://doi.org/10.1016/j.neuroimage.2017.10.003.
Panda, R., Thibaut, A., Lopez-Gonzalez, A., Escrichs, A., Bahri, M.A., Hillebrand, A., Deco, G., Laureys, S., Gosseries, O., Annen, J., Tewarie, P., 2022. Disruption in structural–functional network repertoire and time-resolved subcortical fronto-temporoparietal connectivity in disorders of consciousness. Elife 11, 1–19. https://doi.org/10.7554/eLife.77462.
Piarulli, A., Bergamasco, M., Thibaut, A., Cologan, V., Gosseries, O., Laureys, S., 2016. EEG ultradian rhythmicity differences in disorders of consciousness during wakefulness. J. Neurol. 263, 1746–1760. https://doi.org/10.1007/s00415-016-8196-y.
Posner, J.B., Saper, C.B., Schiff, N., Plum, F., 2008. Plum and Posner's Diagnosis of Stupor and Coma. Oxford University Press. https://doi.org/10.1093/med/9780195321319.001.0001.
Raimondo, F., Rohaut, B., Demertzi, A., Valente, M., Engemann, D.A., Salti, M., Fernandez Slezak, D., Naccache, L., Sitt, J.D., 2017. Brain–heart interactions reveal consciousness in noncommunicating patients. Ann. Neurol. 82, 578–591. https://doi.org/10.1002/ana.25045.
Ramirez-Mahaluf, J.P., Medel, V., Tepper, Á., Alliende, L.M., Sato, J.R., Ossandon, T., Crossley, N.A., 2020. Transitions between human functional brain networks reveal complex, cost-efficient and behaviorally-relevant temporal paths. Neuroimage 219, 117027. https://doi.org/10.1016/j.neuroimage.2020.117027.
Sarasso, S., Casali, A.G., Casarotto, S., Rosanova, M., Sinigaglia, C., Massimini, M., 2021. Consciousness and complexity: a consilience of evidence. Neurosci. Conscious. 2021, 1–24. https://doi.org/10.1093/nc/niab023.
Schiff, N.D., Nauvel, T., Victor, J.D., 2014. Large-scale brain dynamics in disorders of consciousness. Curr. Opin. Neurobiol. 25, 7–14. https://doi.org/10.1016/j.conb.2013.10.007.
Schnakers, C., Giacino, J.T., Løvstad, M., Habbal, D., Boly, M., Di, H., Majerus, S., Laureys, S., 2015. Preserved covert cognition in noncommunicative patients with severe brain injury? Neurorehabil. Neural Repair 29, 308–317. https://doi.org/10.1177/1545968314547767.
Schnakers, C., Hirsch, M., Noé, E., Llorens, R., Lejeune, N., Veeramuthu, V., De Marco, S., Demertzi, A., Duclos, C., Morrissey, A.-M., Chatelle, C., Estraneo, A., 2020. Covert cognition in disorders of consciousness: a meta-analysis. Brain Sci. 10, 930. https://doi.org/10.3390/brainsci10120930.
Seel, R.T., Sherer, M., Whyte, J., Katz, D.I., Giacino, J.T., Rosenbaum, A.M., Hammond, F.M., Kalmar, K., Pape, T.L.-B., Zafonte, R., Biester, R.C., Kaelin, D., Kean, J., Zasler, N., 2010. Assessment scales for disorders of consciousness: evidence-based recommendations for clinical practice and research. Arch. Phys. Med. Rehabil. 91, 1795–1813. https://doi.org/10.1016/j.apmr.2010.07.218.
Sitt, J.D., King, J.R., El Karoui, I., Rohaut, B., Faugeras, F., Gramfort, A., Cohen, L., Sigman, M., Dehaene, S., Naccache, L., 2014. Large scale screening of neural signatures of consciousness in patients in a vegetative or minimally conscious state. Brain 137, 2258–2270. https://doi.org/10.1093/brain/awu141.
Stender, J., Gosseries, O., Bruno, M.A., Charland-Verville, V., Vanhaudenhuyse, A., Demertzi, A., Chatelle, C., Thonnard, M., Thibaut, A., Heine, L., Soddu, A., Boly, M., Schnakers, C., Gjedde, A., Laureys, S., 2014. Diagnostic precision of PET imaging and functional MRI in disorders of consciousness: a clinical validation study. Lancet 384, 514–522. https://doi.org/10.1016/S0140-6736(14)60042-8.

Tadel, F., Baillet, S., Mosher, J.C., Pantazis, D., Leahy, R.M., 2011. Brainstorm: a user-friendly application for MEG/EEG analysis. Comput. Intell. Neurosci. 2011, 1–13. https://doi.org/10.1155/2011/879716.

Tewarie, P., Liuzzi, L., O'Neill, G.C., Quinn, A.J., Griffa, A., Woolrich, M.W., Stam, C.J., Hillebrand, A., Brookes, M.J., 2019. Tracking dynamic brain networks using high temporal resolution MEG measures of functional connectivity. Neuroimage 200, 38–50. https://doi.org/10.1016/j.neuroimage.2019.06.006.

Thibaut, A., Panda, R., Annen, J., Sanz, L.R.D., Naccache, L., Martial, C., Chatelle, C., Aubinet, C., Bonin, E.A.C., Barra, A., Briand, M., Cecconi, B., Wannez, S., Stender, J., Laureys, S., Gosseries, O., 2021. Preservation of brain activity in unresponsive patients identifies MCS star. Ann. Neurol. 90, 89–100. https://doi.org/10.1002/ana.26095.

Todorovic, A., Schoffelen, J.-M., van Ede, F., Maris, E., de Lange, F.P., 2015. Temporal expectation and attention jointly modulate auditory oscillatory activity in the beta band. PLoS ONE 10, e0120288. https://doi.org/10.1371/journal.pone.0120288.

Tzourio-Mazoyer, N., Landeau, B., Papathanassiou, D., Crivello, F., Etard, O., Delcroix, N., Mazoyer, B., Joliot, M., 2002. Automated anatomical labeling of activations in SPM using a macroscopic anatomical parcellation of the MNI MRI single-subject brain. Neuroimage 15, 273–289. https://doi.org/10.1006/nimg.2001.0978.

van der Lande, G.J.M., Casas-Torremocha, D., Manasanch, A., Dalla Porta, L., Gosseries, O., Alnagger, N., Barra, A., Mejías, J.F., Panda, R., Riefolo, F., Thibaut, A., Bonhomme, V., Thirion, B., Clasca, F., Gorostiza, P., Sanchez-Vives, M.V., Deco, G., Laureys, S., Zamora-López, G., Annen, J., 2024. Brain state identification and neuromodulation to promote recovery of consciousness. Brain Commun. https://doi.org/10.1093/braincomms/fcae362.

Vidaurre, D., Hunt, L.T., Quinn, A.J., Hunt, B.A.E., Brookes, M.J., Nobre, A.C., Woolrich, M.W., 2018. Spontaneous cortical activity transiently organises into frequency specific phase-coupling networks. Nat. Commun. 9, 2987. https://doi.org/10.1038/s41467-018-05316-z.

Vohryzek, J., Deco, G., Cessac, B., Kringelbach, M.L., Cabral, J., 2020. Ghost attractors in spontaneous brain activity: recurrent excursions into functionally-relevant BOLD phase-locking states. Front. Syst. Neurosci. 14, 1–15. https://doi.org/10.3389/fnsys.2020.00020.

von Wegner, F., Wiemers, M., Hermann, G., Tödt, I., Tagliazucchi, E., Laufs, H., 2024. Complexity measures for EEG microstate sequences: concepts and algorithms. Brain Topogr. 37, 296–311. https://doi.org/10.1007/s10548-023-01006-2.

Waschke, L., Kloosterman, N.A., Obleser, J., Garrett, D.D., 2021. Behavior needs neural variability. Neuron 109, 751–766. https://doi.org/10.1016/j.neuron.2021.01.023.

Webber, C., Zbilut, J., 2005. Recurrence quantification analysis of nonlinear dynamical systems. Tutorials in Contemporary Nonlinear Methods for the Behavioral Sciences, pp. 26–94.

Xia, M., Wang, J., He, Y., 2013. BrainNet Viewer: a network visualization tool for Human Brain connectomics. PLoS ONE 8. https://doi.org/10.1371/journal.pone.0068910.

Zalesky, A., Fornito, A., Cocchi, L., Gollo, L.L., Breakspear, M., 2014. Time-resolved resting-state brain networks. Proc. Natl. Acad. Sci. 111, 10341–10346. https://doi.org/10.1073/pnas.1400181111.

Zasler, N.D., Aloisi, M., Contrada, M., Formisano, R., 2019. Disorders of consciousness terminology: history, evolution and future directions. Brain Inj. 33, 1684–1689. https://doi.org/10.1080/02699052.2019.1656821.